analytical chemistry

pubs.acs.org/ac

Article

Aptamer-Based Fentanyl Detection in Biological Fluids

Juan Canoura, Yingzhu Liu, Obtin Alkhamis, and Yi Xiao*

Cite This: *Anal. Chem.* 2023, 95, 18258−18267

Read Online

ACCESS | Metrics & More | Article Recommendations | Supporting Information

ABSTRACT: Fentanyl is a widely abused analgesic and anesthetic drug with a narrow therapeutic window that creates easy opportunities for overdose and death. Rapid, accurate, and sensitive fentanyl detection in biosamples is crucial for therapeutic drug monitoring and overdose diagnosis. Unfortunately, current methods are limited to either sophisticated laboratory-based tests or antibody-based immunoassays, which are prone to false results and are mainly used with urine samples. Here, we have utilized library-immobilized SELEX to isolate new aptamers—nucleic acid−based bioreceptors that are well-suited for biosensing—that can specifically bind fentanyl under physiological conditions. We isolated multiple aptamers with nanomolar affinity and excellent specificity against dozens of interferents and incorporated one of these into an electrochemical aptamer-based sensor that can rapidly detect fentanyl at clinically relevant concentrations in 50% diluted serum, urine, and saliva. Given the excellent performance of these sensors, we believe that they could serve as the basis for point-of-care devices for monitoring fentanyl during medical procedures and determining fentanyl overdose.

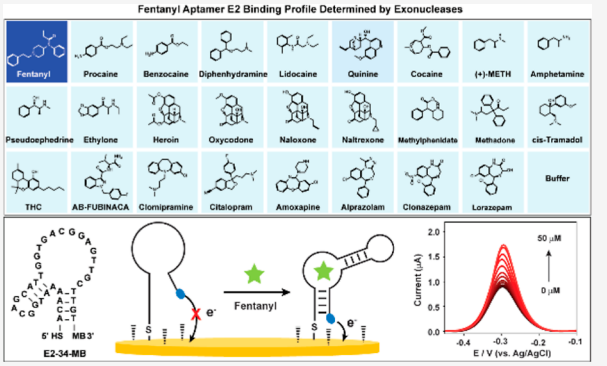

INTRODUCTION

Opioids are among the most frequently prescribed medications in the United States.[1] One of the most commonly employed opioid drugs is the synthetic opioid fentanyl, which is used in critical care for sedation and pain management during surgery, intubation, or in other contexts where relief for severe pain is needed.[2] Fentanyl is also prescribed as an analgesic for discharged patients.[3] The popularity of fentanyl can be attributed to its simple synthesis, low cost, and high potency, which allows for low dosing.[4] Fentanyl activates the μ-opioid receptor to provide pain relief with ∼66-fold greater potency than morphine.[5] Dosing fentanyl is challenging, as its high potency leads to a narrow therapeutic window,[6] requiring careful drug monitoring to maintain therapeutic effects while minimizing dangerous side effects—most critically, respiratory depression.[7] Analgesia typically employs serum concentrations of fentanyl ranging from 0.6−7 nM,[8] while 30−90 nM serum fentanyl is associated with anesthetic effects.[9] Reaching and maintaining therapeutic levels of fentanyl are typically accomplished using general dosing recommendations for relatively healthy patients, but dosing is problematic for infants (<1 year), elderly patients (>50 years), and especially in those with life-threatening conditions such as morbid obesity, kidney failure, sepsis, or cardiovascular disease. Improper dosing in this context can create high risk of mortality.[10] Moreover, in recent years, fentanyl has been increasingly abused for recreational purposes and is a primary contributor to the opioid crisis in the United States.[11] It is frequently used as an adulterant in illicit substances such as heroin, cocaine, and methamphetamine and is even used as a primary drug of abuse. As a result, fentanyl is the fourth most abused drug and the number one cause for drug-related overdose deaths in the United States.[12]

Given the narrow therapeutic window of fentanyl, as well as its complex and rapid pharmacokinetics and toxicokinetics,[13] there is a critical need for assays and tools that enable rapid and simple measurement of this drug in biological samples. Current approaches based on liquid chromatography−mass spectrometry require sample pretreatment and trained personnel, and are limited to specialized laboratory settings.[14] Immunoassays are a promising alternative given their great sensitivity, and several enzyme-linked immunosorbent assays (ELISAs) are currently available for use with oral fluid, blood, and urine. These assays detect fentanyl with limits of detection (LODs) ranging from 0.9−3 nM,[15,16] but they are time-consuming to perform, requiring at least 30−60 min to obtain results, which is far slower than the onset of the fentanyl toxidrome.[7] As an alternative, lateral-flow immunoassays allow for rapid on-site detection of fentanyl within 5 min, albeit with reduced sensitivity (30−600 nM). However, these assays have been shown to cross-react with nonopioid interferents,

Received: September 12, 2023
Revised: November 2, 2023
Accepted: November 16, 2023
Published: November 30, 2023

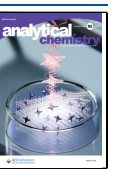

including 3,4-methylenedioxymethamphetamine (MDMA), methamphetamine, and diphenhydramine.[17] Therefore, there remains a need for fentanyl assays that are rapid, sensitive, and specific and which can detect fentanyl in several different biological matrices (e.g., serum, saliva, and urine)—ideally, in on-site or point-of-care settings.

Aptamers are DNA molecules isolated to bind specific targets in vitro via systematic evolution of ligands by exponential enrichment (SELEX).[18,19] They have several advantages over antibodies, including low cost, ease of modification via chemical synthesis, tunable binding profiles, reversible denaturation, and simplicity of engineering to introduce reporting functionality.[20,21] This has led to the development of several aptamer-based sensors capable of rapid, sensitive, and specific detection of small-molecule analytes in various biofluids such as whole blood and serum.[22−24] Here, we have implemented library-immobilized SELEX to isolate high affinity fentanyl-binding aptamers under ionic conditions mimicking biological samples, and using a broad-range of structurally similar interferents for counter-selection. Based on recent work from our group,[25] we have also employed selection pressure to isolate high-affinity aptamers by greatly reducing target concentrations over several rounds. After selection and sequencing, we characterized the binding affinity of the most highly enriched aptamer candidates using isothermal titration calorimetry (ITC) and assessed their target affinity and specificity using an exonuclease-based fluorescence assay.[26,27] Finally, we used one of the isolated aptamers to fabricate an electrochemical aptamer-based (E-AB) sensor that was capable of detecting fentanyl within seconds with a LOD of 10 nM in 50% serum, urine, and saliva. We believe these sensors have potential utility for the detection of recent fentanyl use in saliva, compliance monitoring of fentanyl in urine, and detection of fentanyl in serum for guiding the dosing of challenging patients and assessing drug overdose.

EXPERIMENTAL SECTION

Chemicals and Oligonucleotides. Exonuclease I (Exo I; *E. coli*, 20 U/μL) and Exonuclease III (Exo III; *E. coli*, 100 U/μL) were purchased from New England Biolabs. Alprazolam, (±)-*threo*-methylphenidate hydrochloride (HCl), lorazepam, clonazepam, *cis*-tramadol HCl, (±)-methadone HCl, ethylone HCl polymorph B, fentanyl HCl, heroin HCl, oxycodone HCl, Δ^9-tetrahydrocannabinol (THC), AB-FUBINACA, (+)-methamphetamine HCl, and amphetamine HCl were purchased from Cayman Chemicals. Citalopram hydrobromide and amoxapine were purchased from TCI Chemicals. Clomipramine HCl and lidocaine HCl monohydrate were purchased from Alfa Aesar. Chlorpromazine HCl, procaine HCl, quinine hemisulfate monohydrate, diphenhydramine HCl, benzocaine, cocaine HCl, (+)-pseudoephedrine HCl, naloxone HCl, and naltrexone HCl were purchased from Sigma-Aldrich. SYBR Gold was purchased from Invitrogen. Three kDa cutoff spin filters were purchased from Millipore Sigma, and 800 μL microgravity columns were purchased from Bio-Rad. QIAquick PCR purification kits were purchased from Qiagen. GoTaq Hot Start Colorless Master Mix was purchased from Promega. Formamide, human serum (normal pool), Nunc 384-well black plates, and streptavidin-modified agarose beads were purchased from Thermo Fisher Scientific. 10× phosphate buffered saline (PBS; 46−013-CM, molecular biology grade) and molecular biology-grade water were purchased from Corning. Unless otherwise specified, all other chemicals were purchased from Sigma-Aldrich. All modified and unmodified oligonucleotides were purchased from Integrated DNA Technologies and dissolved in molecular biology-grade water. The random DNA library was purchased with HPLC purification. 5′-thiolated and 3′-methylene blue (MB)-modified aptamers were purchased with dual HPLC purification and dissolved in 1× TE buffer. DNA sequences employed in this work are shown in Supporting Information Table S1. Deionized (DI) water with a conductivity of 18.2 MΩ × cm was obtained using a Milli-Q EQ 7000 apparatus (Millipore Sigma).

SELEX Procedure. Fentanyl-binding aptamers were isolated using a library-immobilized SELEX protocol with some modifications.[28] 1× SELEX buffer was prepared by diluting 5 mL of 10× PBS and 5 mL of 10 mM $MgCl_2$ to a final volume of 50 mL using molecular biology-grade water. Final buffer concentrations are as follows: 10.10 mM Na_2HPO_4, 1.76 mM KH_2PO_4, 136.89 mM NaCl, 2.68 mM KCl, and 1 mM $MgCl_2$, pH 7.4. The 73-nt library molecules consisted of a random 30-nt domain flanked by two primer-binding sites. The initial library pool for the first round of selection comprised ∼6 × 10^{14} oligonucleotides (1 nmol). The SELEX procedure consisted of library immobilization, washing with selection buffer or counter-targets, elution of target-binding strands, library amplification, and single-stranded DNA generation. Washing volumes and countertarget concentrations were gradually increased throughout selection, while the fentanyl concentration was gradually reduced. For positive selection, the target was added to the column in three 250 μL fractions, and eluted aptamers were subsequently collected and then PCR amplified and subjected to the next round of selection. The binding affinity of certain selection pools was determined using a previously reported gel-elution assay.[29] Selection and counter-selection conditions are detailed in Supporting Information, Tables S2 and S3, respectively.

High-Throughput Sequencing. Rounds 10−13 pools were submitted for high-throughput Illumina sequencing at GENEWIZ. Before submission, Illumina adapters were added to each pool via PCR using a customized forward and reverse primer (Supporting Information, Table S1, Illumina-FP and -RP). Specifically, 10 nM of each pool was mixed with 1 μM Illumina-FP and -RP (final concentrations) and subjected to 10 PCR cycles using the following conditions: 2 min at 95 °C; 9 cycles of 95 °C for 15 s, 58 °C for 30 s, and 72 °C for 45 s; and finally 5 min at 72 °C. PCR product size was confirmed using polyacrylamide gel electrophoresis (PAGE), and the amplified product was purified using the QIAquick PCR purification kit and submitted for HTS. Two fastq files were obtained for each pool, one containing the forward reads and the other the reverse reads. The reverse reads were converted into their reverse complement using the fastx toolkit and combined with the forward reads. Primer sequences were trimmed from fastq files using cutadapt[30] followed by further analysis using FASTAptamer[31] to obtain sequence population data and assess enrichment between selection rounds and clustal omega[32] was used to obtain sequence alignments.

Binding Characterization Using an Exonuclease-Based Fluorescence Assay. The binding profiles of our aptamer candidates were evaluated using a recently published exonuclease fluorescence assay.[26,27] Specifically, 1 μL of aptamer (final concentration = 0.5 μM) was added to 3 μL of Mg^{2+}-free PBS (final concentration = 1×). The solution was heated to 95 °C for 10 min, immediately cooled on ice, and

https://doi.org/10.1021/acs.analchem.3c04104
Anal. Chem. 2023, 95, 18258−18267

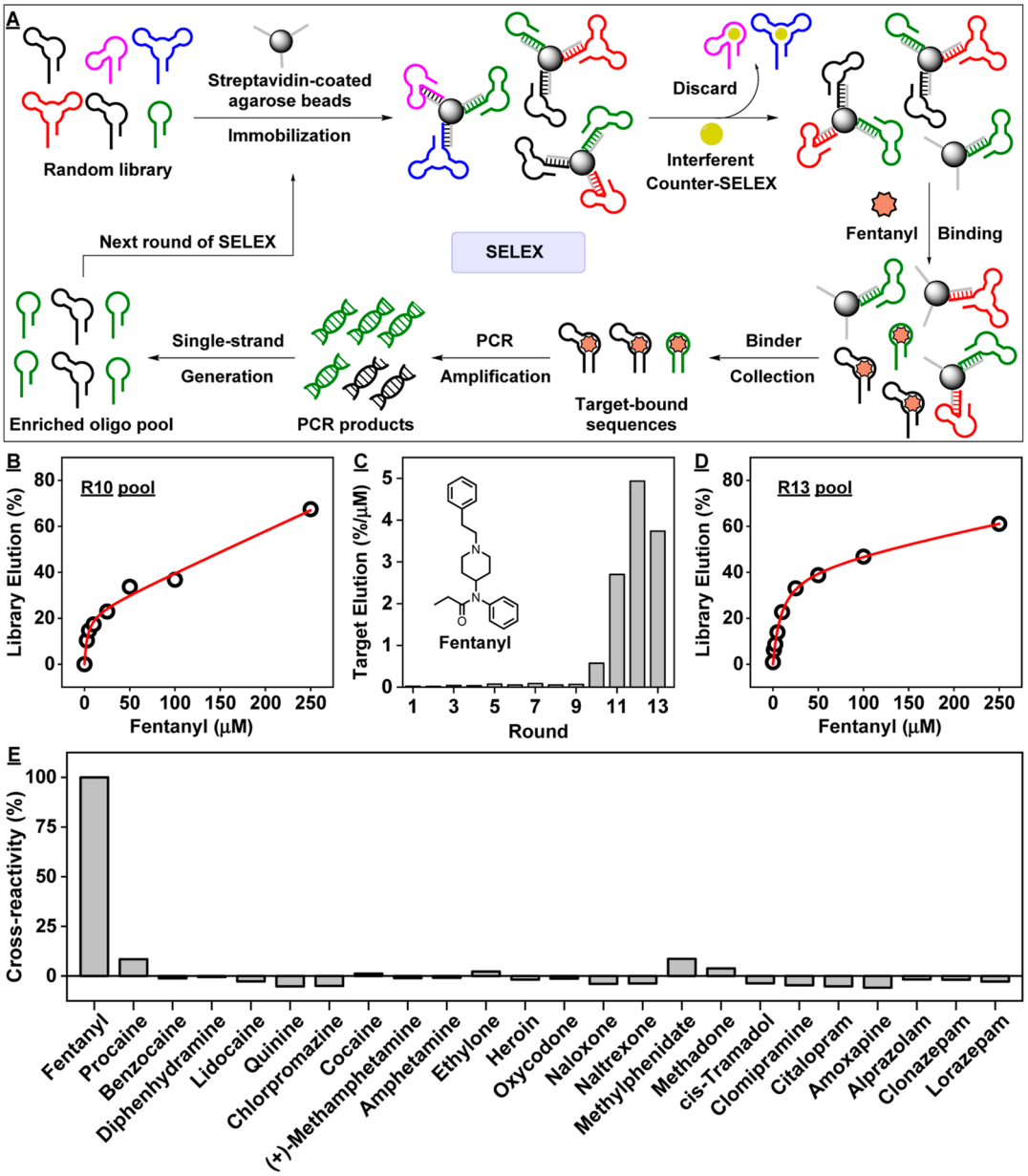

Figure 1. Selection of DNA aptamers that bind to the synthetic opioid fentanyl under physiological conditions. (A) Scheme of the library-immobilized SELEX process. (B) Affinity of the round 10 pool, as determined by a gel-elution assay. (C) The percentage of pool eluted each round per concentration of fentanyl. (D) Affinity of the round 13 pool, as determined by a gel-elution assay. Note that the binding curves in panels B and D suggest the presence of two distinct populations of aptamers with divergent affinities; as such, all binding curves were fitted with a modified two-site Langmuir equation, with two K_Ds reported. (E) Specificity of the round 13 pool as determined by the gel elution assay. Cross-reactivity was calculated relative to pool elution by fentanyl. [Fentanyl] = 25 μM, [Interferent] = 250 μM, except for clomipramine, citalopram, alprazolam, amoxapine, lorazepam, and clonazepam (100 μM).

mixed with 0.5 μL of $MgCl_2$ (final concentration = 1 mM) and 0.5 μL of BSA (final concentration = 0.1 mg/mL). Next, 20 μL of buffer either alone or containing fentanyl (final concentration = 25 μM) or various interferents (final concentrations = 10 μM THC or AB-FUBINACA; 50 μM clomipramine, citalopram, amoxapine, alprazolam, clonazepam, or lorazepam; 250 μM benzocaine, procaine, diphenhydramine, lidocaine, quinine, chlorpromazine, cocaine, (+)-methamphetamine, amphetamine, (+)-pseudoephedrine, ethylone, heroin, oxycodone, naloxone, naltrexone, methylphenidate, methadone, or tramadol) was added and incubated at 25 °C for 30 min. Then, 25 μL of exonuclease mixture (final concentrations = 0.025 U/μL Exo III and 0.05 U/μL Exo I) dissolved in 1× buffer containing 0.1 mg/mL BSA was added and incubated at 25 °C; digestion progress was monitored by collecting 5 μL samples at various time points and mixing these with 30 μL of quench solution (final concentrations = 1.76 mM KH_2PO_4, 10.10 mM Na_2HPO_4, 136.89 mM NaCl, 2.68 mM KCl, 12.5% formamide, 10 mM EDTA, 1× SYBR Gold, pH 7.4) in the wells of a Nunc 384-well black plate. Fluorescence intensity of SYBR Gold ($\lambda_{ex}/\lambda_{em}$ = 495/537 nm) was recorded by using a Tecan Spark microplate reader. Enzymatic inhibition was calculated as resistance value (R_{value}).[33] Specifically, the area under the curve (AUC) of the digestion time-course was calculated in the absence and presence of the target where R_{value} = (AUC_{target}/AUC_{blank}) − 1.

https://doi.org/10.1021/acs.analchem.3c04104
Anal. Chem. 2023, 95, 18258−18267

Determination of Aptamer Binding Affinity Using ITC. All ITC experiments were performed at 23 °C in 1× PBS buffer with 1 mM $MgCl_2$ using a MicroCal ITC200 instrument (Malvern). For each experiment, the aptamer dissolved in buffer was heated at 95 °C for 10 min and then immediately cooled on ice, followed by the addition of $MgCl_2$. The sample cell was loaded with 300 μL of aptamer solution. Fentanyl was dissolved in 1× PBS buffer with 1 mM $MgCl_2$ and loaded into the syringe. The concentrations of aptamer and fentanyl used for each experiment are listed in Supporting Information, Table S4. Typically, each titration began with a 0.4 μL purge injection, followed by 19 injections of 2 μL with 180 s spacing between injections. The spacing between injections and the number of injections was altered for certain aptamers as necessary. Correction was performed on the raw data to account for the dilution heat. The corrected data were analyzed using Origin 7 with the MicroCal analysis kit and fitted using a single-site binding model.

Fabrication of E-AB Sensors. E-AB sensors were fabricated using a 5′-thiolated, 3′-methylene blue (MB)-modified E2−34 aptamer (E2−34-MB) with a target-assisted immobilization strategy.[34] First, the gold disk electrodes (2 mm diameter, CHI Instruments) were polished and electrochemically cleaned using a previously reported method.[35] To prepare the aptamer for electrode modification, the disulfide group on E2−34-MB was reduced by incubating it in 100 mM Tris(2-carboxyethyl)phosphine hydrochloride solution for 2 h at room temperature in the dark. The freshly reduced aptamer was diluted to various concentrations in 1× PBS with 1 mM $MgCl_2$ containing 50 μM fentanyl. The cleaned electrodes were rinsed with distilled water, dried with nitrogen, and immediately immersed in a solution of the aptamer−target complex overnight in the dark at room temperature. The aptamer-modified electrodes were then backfilled with 1 mM 6-mercapto-1-hexanol in 1× PBS with 1 mM $MgCl_2$ containing 50 μM fentanyl for 2 h at room temperature. Finally, the E2−34-MB-modified electrodes were thoroughly washed with deionized water and stored in 1× PBS with 1 mM $MgCl_2$ before use.

Optimization of E-AB Sensor Performance. All electrochemical measurements were performed using the CHI760D electrochemical workstation and a three-electrode system, including an E2−34-MB-modified gold working electrode, a platinum counter electrode (CHI Instruments), and a Ag/AgCl reference electrode (CHI Instruments). Square-wave voltammetry (SWV) was utilized for the measurements (parameters: scan range −0.1 to 0.45 V, scan rate 200 Hz, amplitude 25 mV, increment 1 mV). Signal gains were calculated using the equation: $(I_T - I_0)/I_0 \times 100\%$, in which I_T and I_0 represent the peak currents in the presence and absence of target, respectively. The measurement frequency was first optimized using the modified electrode in the range 25−600 Hz in the absence and presence of 25 μM fentanyl. To investigate the effect of aptamer surface coverage on sensor signal, we fabricated gold working electrodes with various concentrations of E2−34-MB (50, 100, or 200 nM) and measured their surface coverage using the Tarlov method.[36] Sensor performance was evaluated by testing 0.1, 1, and 25 μM fentanyl at a frequency of 200 Hz.

Detection of Fentanyl in Buffer, 50% Urine, 50% Saliva, and 50% Serum and Specificity Testing. For fentanyl detection in buffer, the E2−34-MB-fabricated E-AB sensors were challenged with 0−50 μM fentanyl in 1× PBS with 1 mM $MgCl_2$. For detection in biosamples, urine and saliva pools were collected using a previously reported protocol.[37] 50% urine, saliva, or serum were prepared by mixing 2× PBS with 2 mM $MgCl_2$ with pooled human urine, saliva, or serum at a 1:1 ratio (v/v). Different concentrations of fentanyl were then spiked into diluted urine, saliva, or serum. For specificity testing, most interferents were prepared at a final concentration of 100 μM in 1× PBS with 1 mM $MgCl_2$. However, clomipramine, citalopram, alprazolam, amoxapine, lorazepam, and clonazepam were prepared in 1× PBS with 1 mM $MgCl_2$ containing 1% methanol with a final concentration of 50 μM due to solubility limitations. SWV spectra were recorded for all samples, and the peak current was used to calculate the signal gain. Cross-reactivities of the interferents were calculated against the signal gain from 10 μM fentanyl. All experimental data were reported as the average results from three independent working electrodes. Error bars represent the standard deviation for the three working electrodes for each measurement.

RESULTS AND DISCUSSION

Initial SELEX for Isolation of Fentanyl-Binding Aptamers. We performed library-immobilized SELEX with a 73-nucleotide (nt) stem-loop-structured DNA library[38] (Supporting Information, Table S1) using fentanyl as the target. The library is composed of a 30-nt random region serving as the putative binding domain, an 8-base-pair (bp) stem, and two PCR primer sites. The library sequences also contained a fixed-sequence region that can hybridize with a biotinylated complementary 15-nt DNA (Bio-cDNA) to enable library immobilization on streptavidin-coated agarose beads. When the target is added, library strands that bind to the target undergo a conformational change and are released into solution. These sequences are then collected and amplified for another round of selection (Figure 1A).

To isolate aptamers that bind to fentanyl optimally in serum, we performed SELEX in 1× PBS (pH 7.4) with 1 mM $MgCl_2$, which mimics biological pH and ionic strength. Details on the employed selection conditions and strategies are provided in Supporting Information, Tables S2 and S3. We began with 1 nmol of the library (10^{14} unique sequences) and used 100 μM fentanyl to elute target binders in the first round of selection. For the second and third rounds, we used 350 pmol library and 100 μM fentanyl, with counter-SELEX against a variety of interferents (SI, Figure S1) at concentrations ranging between 100−250 μM. These interferents included cutting agents and adulterants (e.g., procaine, lidocaine, quinine, benzocaine, diphenhydramine, and chlorpromazine), pharmaceuticals (e.g., methadone, tramadol, amoxapine, clomipramine, methylphenidate, naloxone, naltrexone, citalopram, oxycodone, lorazepam, alprazolam, and clonazepam), and illicit substances (e.g., amphetamine, cocaine, (+)-methamphetamine, heroin, and ethylone). Most counter-targets were used individually, while others were employed in groups (Supporting Information, Table S3). To increase the stringency, we lowered the concentration of fentanyl to 50 μM in the fourth round. Until round 10, the proportion of the pool eluted by fentanyl remained consistent at around 0.7−2.6%. This is in contrast to the relatively large amount of pool eluted by certain countertargets (2−8%) such as clomipramine, alprazolam, clonazepam, citalopram, diphenhydramine, lidocaine, and benzocaine (data not shown). In the tenth round, the proportion of fentanyl-eluted pool dramatically increased to

https://doi.org/10.1021/acs.analchem.3c04104
Anal. Chem. 2023, 95, 18258−18267

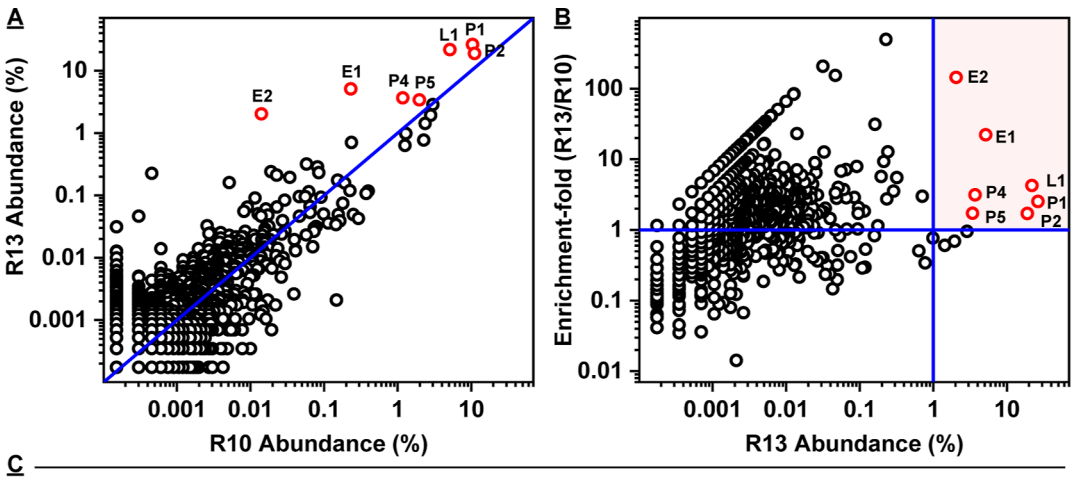

C

Aptamer ID	Sequence (5′ – 3′)	K_D (nM)
E1	GGGACGACTGCTTGGGTAGGTCGGGCTTGGGTTCGGCGGTCGTCCC	79 ± 7
E2	GGGACGACAAAATGGCAGCATTGGTGACGGAGTTGCTTGTCGTCCC	143 ± 13
L1	GGGACGACAAAAATGGAAGCATTGGTTGTTGGTGCTTTGTCGTCCC	426 ± 20
P1	GGGACGACAGCTTGGTTTGGTCGGGGTAGGGTTCGGATGTCGTCCC	97 ± 6
P2	GGGACGACTAATGGGAGCATTGGTCCACGCAGTGTGCAGTCGTCCC	268 ± 8
P4	GGGACGACGGTTGGCTTGGGGTCGGGTGTGGGTGCGGCGTCGTCCC	49 ± 3
P5	GGGACGACTGCTTGGGTAGGTCGGGTTTGGGTTCGGCGGTCGTCCC	128 ± 5

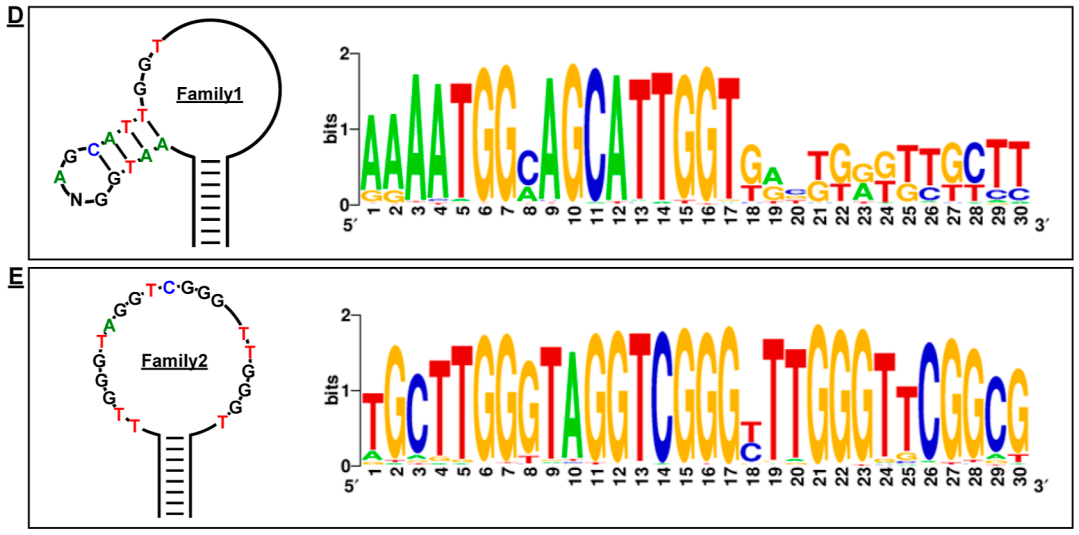

Figure 2. Analysis of HTS data of pools from fentanyl SELEX. (A) Sequence abundance in the round 10 and 13 pools. Each black circle represents a unique sequence, and sequences above or below the blue diagnol line respectively exhibited positive or negative enrichment between the two rounds. (B) Enrichment-fold of each sequence between rounds 10 and 13, plotted against that sequence's abundance in round 13. Red circles show sequences with both >1% abundance and >1 enrichment fold, which were selected for further analysis. (C) Sequences and ITC-derived fentanyl-binding affinities of the selected aptamers. (D,E) Secondary structures and sequence logos of isolated fentanyl binding aptamers from (D) AT-rich Family 1 and (E) GT-rich Family 2. Sequence alignments were identified using clustal-omega software and a sequence logo was constructed using WebLogo.[39]

8.7%, indicating that the pool was enriched with aptamers that bound to this target, while pool elution by all counter-targets was greatly decreased (0.3−4%) except for alprazolam, which remained at ∼6% (data not shown). We then used a previously reported gel elution assay[29] to determine the fentanyl-binding affinity and specificity of this round 10 pool. The pool demonstrated a distinct biphasic binding profile, with one population of sequences binding strongly to fentanyl with a dissociation constant (K_D) of 2 μM and another population with a much higher K_D of ∼1 mM (Figure 1B). Minimal cross-reactivity was observed to all counter-targets except for procaine and methylphenidate (∼10%) (Supporting Information, Figure S2). This binding behavior indicated that the round 10 pool consisted of low- and moderate-affinity binders (>40%) with a minority of high-affinity binders (<20%).

In our recent work,[25] we determined that the concentration of target in initial rounds of SELEX and the degree at which target concentration is decreased throughout the selection rounds is crucial for enriching high-affinity aptamers. Since binders make up a relatively small proportion of the library during the early rounds of SELEX, it is preferable to use enough target to mitigate the loss of such binders. Thereafter in later rounds, when binder concentrations are higher, target concentrations can be lowered to increase the selection stringency. Therefore, we posited that high-affinity fentanyl aptamers could be preferentially enriched by greatly reducing

https://doi.org/10.1021/acs.analchem.3c04104
Anal. Chem. 2023, 95, 18258−18267

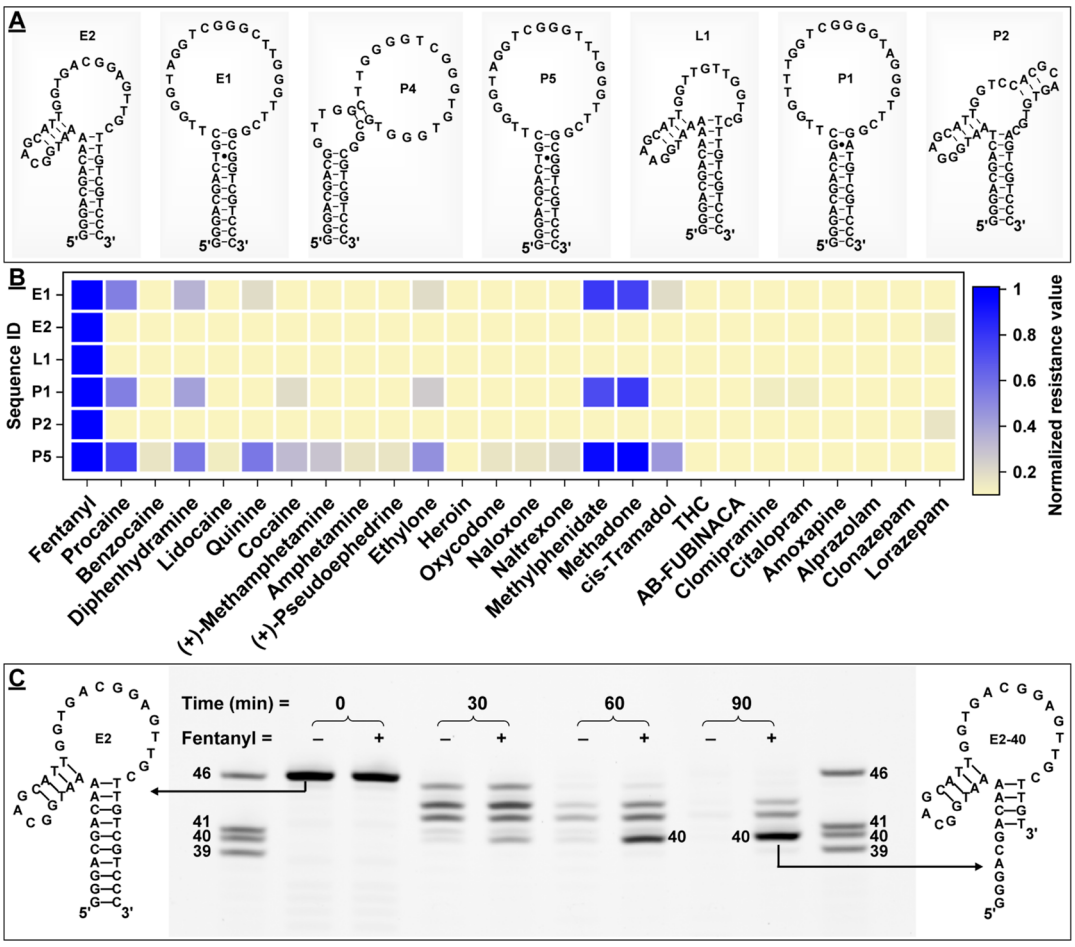

Figure 3. Assessing the affinity and specificity of fentanyl aptamers and identification of an optimal candidate for E-AB sensor fabrication. (A) NUPACK[42]-predicted secondary structure of aptamer candidates. (B) Normalized resistance values of six fentanyl aptamers in the presence of 25 μM fentanyl or various interferents. Resistance values are normalized by using fentanyl for each sequence individually. (C) PAGE analysis of a time-course digestion of E2 with 250 μM fentanyl. NUPACK[42]-predicted secondary structures of parent aptamer E2 and hypothetical structure of the major digestion product E2−40 are provided at left and right, respectively.

the target concentration within a few rounds. Thus, for the 11th round, we used 10 μM fentanyl to perform SELEX. Despite the increased selection stringency, 8.1% of the pool was eluted. To further increase stringency in the 12th round, we decreased the target concentration to 5 μM but still observed a largely similar pool elution of 7.4%. We then performed one more round of selection using the same target concentration and obtained a pool elution of 5.6% (Figure 1C). We performed the gel-elution assay to determine the affinity of the resulting pool and again observed a biphasic binding profile in which one population of sequences bound strongly to fentanyl with a K_D of 8 μM while another population bound with a much higher K_D of ∼1 mM (Figure 1D). Nevertheless, the population of high-affinity aptamers had increased from ∼15% in round 10 to 40% in round 13. Clearly, the increase in stringency promoted the enrichment of high affinity aptamers. We further assessed the specificity of this pool and observed <5% cross-reactivity against all counter-targets (Figure 1D and Supporting Information, Figure S3). We therefore concluded that we had obtained aptamers with sufficient affinity and specificity for fentanyl by this stage of SELEX.

High-Throughput Sequencing of SELEX Pools and Aptamer Characterization Using ITC. To identify aptamer candidates, we performed HTS analysis of the round 10−13 pools. The overall diversity of the pools decreased as SELEX progressed, from 22.1% unique sequences in the 10th round to 9.6% in round 11, 2.1% in round 12, and 1.2% in the 13th round (Supporting Information, Figure S4). To select candidate aptamers, we first plotted the population of each sequence in rounds 10 and 13 in a 2D coordinate system to depict the relative shift in population between the two rounds (Figure 2A). From this data, it is apparent there were several aptamers that were highly abundant and/or highly enriched. We then plotted the sequence abundance in round 13 against the fold-enrichment in population growth between rounds 10 and 13, and chose seven sequences (E2, E1, P4, P5, L1, P1, and P2) that had abundance >1% and enrichment-fold >1 (Figure 2B). We synthesized these aptamers and utilized ITC to determine their K_D values for fentanyl. These candidates exhibited affinities ranging from 49−426 nM (Figure 2C; Supporting Information, Table S4 and Figures S5 and S6). Clustering of the sequences for these seven aptamers revealed two different families. Sequences in Family 1 (E2, P2, and L1) contained a two-way junction structure with an AT-rich hairpin loop and a variable bulge (Figure 2D), while those in Family 2 (E1, P1, P4, and P5) were GT-rich (Figure 2E).

https://doi.org/10.1021/acs.analchem.3c04104
Anal. Chem. 2023, 95, 18258−18267

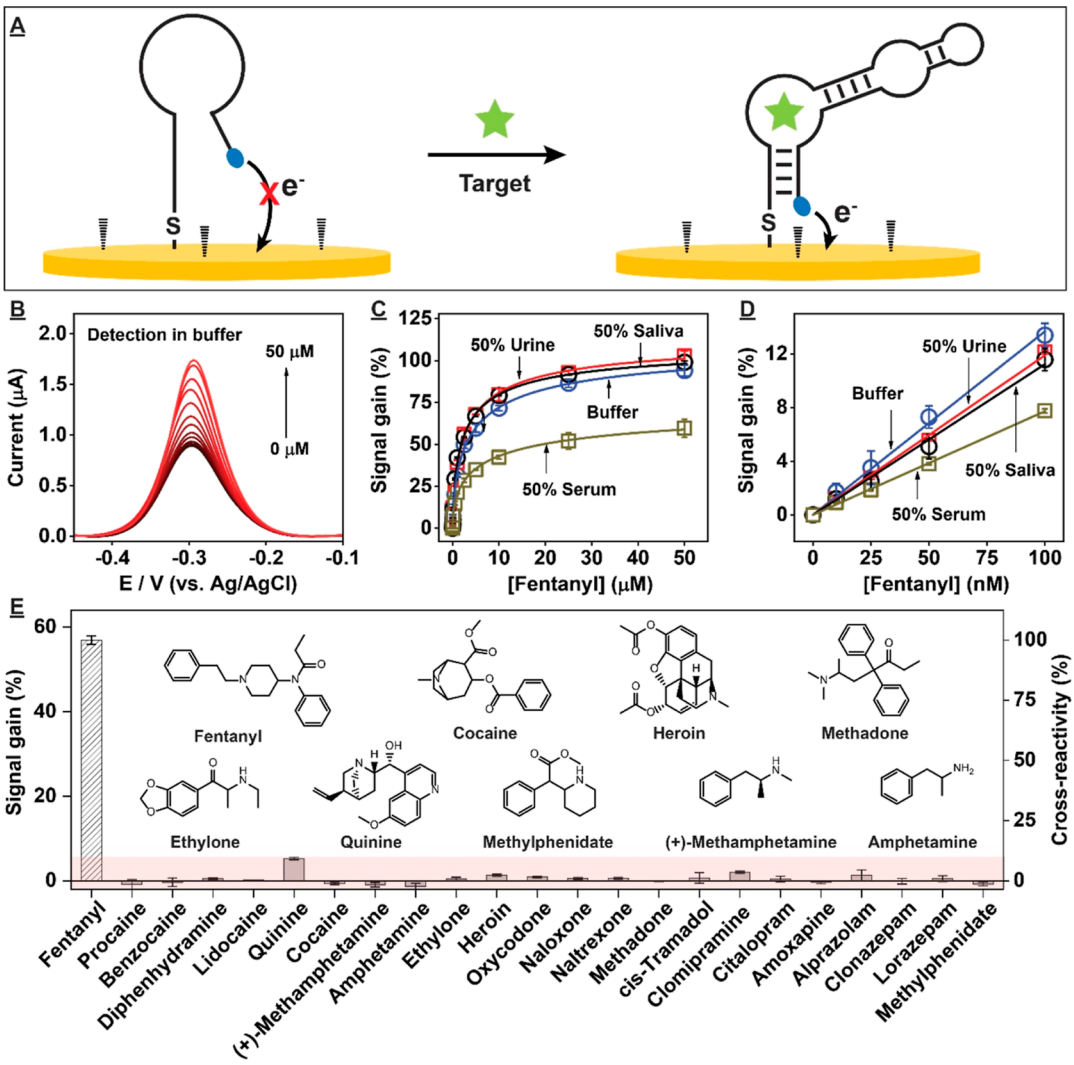

Figure 4. Detection of fentanyl was performed using E-AB sensors fabricated with E2−34-MB. (A) E-AB sensors consist of an aptamer tagged with methylene blue covalently bound to a gold electrode surface. Target binding to the aptamer causes the aptamer to undergo a conformational change, which alters the distance of the methylene blue tag from the electrode surface and hence affects the electric current when scanned via square wave voltammetry. (B) Square wave voltammograms in the presence of various concentrations of fentanyl. (C) Calibration curves for fentanyl detection in buffer (blue), 50% human urine (red), 50% human saliva (black), and 50% human serum (gold), with signals at low target concentrations shown in D. We observed a measurable LOD of 10 nM in all sample matrices. (E) Cross-reactivity of the E-AB sensor to various interferents relative to 10 μM fentanyl, with the red-shaded area representing the threshold of 10% cross-reactivity—signals below this level are considered to be nonspecific background. Error bars represent data from three independently fabricated sensors.

Exonuclease-Guided Aptamer Characterization and Truncation. We next utilized our recently developed exonuclease-based digestion assay to determine aptamer affinity and specificity.[26,27] In this assay, the double-stranded DNA nuclease exonuclease III (Exo III) and single-stranded DNA nuclease exonuclease I (Exo I) digest aptamers from the 3′ terminus into mononucleotides in the absence of the target but are unable to digest the aptamer beyond a certain point in the presence of target, typically yielding a single major truncation product. The resistance of the aptamer to enzymatic digestion is proportional to the affinity of this truncation product for its target,[27] and the resulting truncated product typically has structure-switching functionality,[40] making it a potentially useful receptor for the subsequent development of folding-based aptamer sensors.[41]

We digested our seven aptamer candidates (Figure 3A) in the presence of 0, 25, or 250 μM fentanyl and monitored digestion by taking aliquots of the reaction mixture at various times, staining with the DNA-binding dye SYBR Gold, and measuring the resulting fluorescence (Supporting Information, Figures S7). Aptamers that bound to fentanyl tightly retained higher fluorescence in the presence of the target over the whole time-course. We then analyzed the digestion kinetics using the AUC parameter,[33] and used this to compute the resistance value (R_{value}) as a metric for evaluating aptamer-ligand binding strength, where $R_{value} = (AUC_{target}/AUC_{blank}) - 1$. A greater R_{value} indicates stronger aptamer-ligand binding, whereas a R_{value} of 0 indicates that the aptamer and ligand have no affinity for each other. P1, E1, and E2 had the highest R_{value} for both concentrations of fentanyl, while P2, P5, and L1 had moderate R_{value} (Supporting Information, Figure S8). P4 showed little enzymatic inhibition in the presence of fentanyl, and we therefore omitted this sequence from further testing. We next determined the specificity of the remaining six aptamers against the counter-targets employed in counter-SELEX as well as additional potential interferents (e.g., AB-FUBINACA and

https://doi.org/10.1021/acs.analchem.3c04104
Anal. Chem. 2023, 95, 18258−18267

THC) using the same exonuclease assay (Figure 3B). In general, aptamers from Family 2 (i.e., E1, P1, and P5) displayed cross-reactivity to cocaine, procaine, diphenhydramine, ethylone, methylphenidate, and methadone (Supporting Information, Figure S9). In contrast, Family 1 members had superior specificity; L1, E2, and P2 had <10% cross-reactivity to any tested compound (Supporting Information, Figure S10).

Given that E2 had the best combination of affinity and specificity, we chose this aptamer for further sensor development. First, we determined the identity of its exonuclease truncation product by performing a PAGE analysis of the digested aptamer. We observed that the aptamer was truncated 6 nt from its 3′ end to form a 40-nt product (Figure 3C). Given that overhangs sometimes negatively impact aptamer affinity,[43,44] the remaining 5′ overhang of this aptamer was removed and the 34-nucleotide construct, termed E2−34, was synthesized. Using ITC, we determined E2−34 bound to fentanyl with a K_D of 1207 ± 24 nM, a ∼6-fold higher value than the K_D of the parent aptamer (Supporting Information, Figure S11). We then performed circular dichroism spectroscopy to determine whether the aptamer underwent conformational changes upon target binding (Supporting Information, Figure S12). The aptamer by itself exhibited a broad positive peak spanning 260−290 nm and a negative peak at 250 nm, indicating the presence of B-form DNA.[45] Upon the addition of fentanyl, the positive peak grew in intensity, and its peak shifted to ∼290 nm; the negative peak decreased in intensity, and a new negative peak formed at ∼265 nm. This spectrum is indicative of the formation of an antiparallel G-quadruplex[45] and provides clear confirmation of a fentanyl-binding-induced conformational change.

Development of an E-AB Sensor for Fentanyl Detection in Biological Samples. E-AB sensors[46] are being increasingly used for small-molecule detection in biosamples due to their high selectivity, sensitivity, and rapid response.[23] E-AB sensors are folding-based sensors in which an electrode-bound aptamer is modified at one end with a thiol group and a methylene blue redox tag at its other terminus. Initially, the aptamers are unfolded, which positions the redox tag far from the electrode surface. Aptamer-target binding induces a conformational change, bringing the redox tag closer to the electrode surface and increasing the redox current in a target concentration-dependent manner (Figure 4A). The target binds to the electrode-coupled aptamer, most likely interacting with the SELEX-evolved random domain via some combination of van der Waals interactions, electrostatics, pi−pi stacking, and hydrogen bonding. For our sensor, we synthesized E2−34 with a 3′-methylene blue tag and a 5′-thiol group and utilized this construct (E2−34-MB) to fabricate E-AB sensors. We immobilized E2−34-MB onto a gold working electrode using our previously reported target-assisted immobilization strategy, in which the aptamer is first complexed with the target and then immobilized onto the electrode to provide sufficient spacing for aptamer target-binding and folding.[34] E-AB sensors made using this strategy have improved signal-to-noise ratios and LODs relative to those made using conventional aptamer immobilization approaches.[34]

We first optimized sensor surface coverage by immobilizing different amounts of aptamer on the electrode and found that electrodes with aptamer density of 4.0 pmol/cm^2 yielded the highest signal gain (Supporting Information, Figure S13A). We also optimized square-wave measurement frequency to a final value of 200 Hz in order to maximize signal gain (Supporting Information, Figure S13B). Using these optimized conditions, we challenged the sensor with 0−50 μM fentanyl and observed increased current with increasing target concentrations (Figure 4B), obtaining a linear range from 0−100 nM and a LOD of 10 nM in buffer (Figure 4C,D). Impressively, our sensor demonstrated similar sensing performance in 50% human saliva and human urine, with identical linear ranges, LODs, and maximum signal gain values (Supporting Information, Figures S14A,B). We observed that the SWV peak potentials were quite similar (−0.3 V) for buffer, saliva, and serum, while for urine, the peak potential was at −0.28 V. This is most likely because the pH of urine differs somewhat from that of buffer, saliva, and serum (pH ∼ 7.4). We observed some signal suppression in 50% human serum (Supporting Information, Figure S14C), but the sensor still retained excellent performance with a LOD of 10 nM fentanyl and a robust signal-to-noise ratio (Figure 4C,D). The relative standard deviation for E-AB sensors is typically 1−5%, although there can be variability in this error. The observed differences in the standard deviations for buffer and serum may be due to variables unrelated to the matrix, such as electrode surface roughness or surface coverage. Finally, we assessed the cross-reactivity of the E-AB sensor to 22 different interferents at 5- to 10-fold higher concentrations relative to fentanyl. The sensor exhibited <10% cross-reactivity to all of these interferents, all of which were tested at concentrations well above what would be found in bodily fluids (Figure 4E; Supporting Information, Figures S15−S17). As such, there should be minimal response to interferents present at lower physiologically relevant concentrations than what we used here. These results demonstrate that our E-AB sensor is sufficiently sensitive to detect fentanyl at low concentrations in biological matrices without any meaningful response to interferents. For example, at 100 nM fentanyl, our sensor yields a signal gain of ∼12%, twice as high as that produced by the most cross-reactive interferent: a 1000-fold higher concentration (100 μM) of quinine, which is typically at most 1 μM in bodily fluids.[47] Given that the concentration of fentanyl is generally 10−350 nM in human blood, saliva, or urine in the context of overdose cases,[48,49] our sensor should be suitable for seconds-scale and accurate on-site assessment of recent fentanyl use, fentanyl monitoring during surgical procedures, and overdose in ambulances and emergency departments.

CONCLUSIONS

We describe here the development of a sensitive and specific aptamer-based sensor for the rapid detection of fentanyl in various biological samples. The concentration of fentanyl is typically quite low in matrices, such as blood, saliva, or urine, and successful detection of this drug requires aptamers that can achieve a LOD in the low-nanomolar range. In this work, we used library-immobilized SELEX to isolate aptamers that can bind fentanyl under physiologically relevant conditions. We then utilized HTS analysis to identify aptamer candidates, selecting those that were both relatively abundant in the final pool and underwent rapid growth between selection rounds. We utilized ITC to determine the affinity of the seven most promising aptamers and found that most have a nanomolar affinity for fentanyl. We evaluated the specificity of six of our aptamer candidates against the interferents employed in our counter-SELEX screen using an exonuclease-based fluores-

https://doi.org/10.1021/acs.analchem.3c04104
Anal. Chem. 2023, 95, 18258−18267

cence assay and identified a structurally related family of aptamers (L1, E2, and P2) that exhibited superior specificity toward all tested interferents. Our aptamers' exceptional specificity can be attributed to the fact that we performed an extensive counter-SELEX procedure during the aptamer isolation process, which effectively removes library strands that bind to interferents. We introduced structure-switching functionality into E2—the aptamer that exhibited the best combination of affinity and specificity from that family—and used the resulting E2−34-MB construct to fabricate an E-AB sensor. This sensor produced a robust signal-to-noise ratio with a LOD of 10 nM fentanyl in 50% human urine, serum, and saliva and with minimal response to a wide range of interferents. The fentanyl toxidrome occurs within minutes.[7] Our E-AB sensor takes only a few seconds to provide a result. Therefore, such an E-AB sensor could potentially be employed to assess fentanyl overdoses in a variety of point-of-care settings in a timely manner. By converting the current E-AB sensor to a paper-based device, as we have demonstrated previously,[50] we could further lower the cost of testing without compromising on analytical performance. In the future, these aptamers could potentially even be adapted for use in E-AB sensors for real-time in vivo therapeutic fentanyl monitoring,[51,52] for example, during surgical procedures.

■ ASSOCIATED CONTENT

Supporting Information

The Supporting Information is available free of charge at https://pubs.acs.org/doi/10.1021/acs.analchem.3c04104.

DNA sequences used in this work; SELEX strategy and conditions for isolating fentanyl-binding aptamers; aptamer affinity characterization data via ITC; chemical structures of interferents employed in counter-SELEX; specificity of the round 10, 13 combined pools determined by gel elution assay; high-throughput sequencing (HTS) analysis of pool diversity for rounds 10−13; ITC characterization of fentanyl binding affinity of seven aptamer candidates; exonuclease digestion time-course and resistance values of fentanyl-binding aptamer candidates; screening the specificity of fentanyl-binding aptamers against interferents using an exonuclease digestion assay; characterization of fentanyl-binding affinity of E2−34 using ITC and circular dichroism spectra of E2−34 in the absence and presence of 10 μM fentanyl; optimizing analytical performance of E2−34-MB fabricated electrochemical aptamer-based (E-AB) sensors; SWV data for E2−34-MB modified E-AB sensors in the presence of fentanyl in 50% saliva, urine and serum; SWV spectra collected in buffer with or without interferents; and high-throughput sequencing data for SELEX are deposited in the Sequence Read Archive of the NCBI and can be found using the title of this paper (PDF)

■ AUTHOR INFORMATION

Corresponding Author

Yi Xiao − *Department of Chemistry, North Carolina State University, Raleigh, North Carolina 27607, United States;* orcid.org/0000-0001-7278-9811; Email: yxiao34@ncsu.edu

Authors

Juan Canoura − *Department of Chemistry, North Carolina State University, Raleigh, North Carolina 27607, United States*

Yingzhu Liu − *Department of Chemistry, North Carolina State University, Raleigh, North Carolina 27607, United States*

Obtin Alkhamis − *Department of Chemistry, North Carolina State University, Raleigh, North Carolina 27607, United States*

Complete contact information is available at: https://pubs.acs.org/10.1021/acs.analchem.3c04104

Notes

The authors declare no competing financial interest.

■ ACKNOWLEDGMENTS

This work was supported by the National Institute of Justice, Grant Office of Justice Programs, U.S. Department of Justice Award 2019-DU-BX-0024 and 2022-GG-04440-RESS.

■ REFERENCES

(1) Fuentes, A. V.; Pineda, M. D.; Venkata, K. C. N. *Pharmacy* **2018**, *6*, 43.
(2) Armenian, P.; Vo, K. T.; Barr-Walker, J.; Lynch, K. L. *Neuropharmacology* **2018**, *134*, 121−132.
(3) Clotz, M. A.; Nahata, M. C. *Clin. Pharmacol.* **1991**, *10*, 581−593.
(4) Stanley, T. H. *J. Pain* **2014**, *15*, 1215−1226.
(5) Pereira, J.; Lawlor, P.; Vigano, A.; Dorgan, M.; Bruera, E. *J. Pain Symptom Manage.* **2001**, *22*, P672−P687.
(6) Schmid, C. L.; Kennedy, N. M.; Ross, N. C.; Lovell, K. M.; Yue, Z.; Morgenweck, J.; Cameron, M. D.; Bannister, T. D.; Bohn, L. M. *Cell* **2017**, *171*, 1165−1175.e13.
(7) Stoeckel, H.; Schüttler, J.; Magnussen, H.; Hengstmann, J. H. *Br. J. Anaesth.* **1982**, *54*, 1087−1095.
(8) Peng, P. H.; Sandler, A. N. *Anesthesiology* **1999**, *90*, 576−599.
(9) Hall, R. I.; Molderhauer, C. C.; Hug, C. C. *Anesth. Analg.* **1993**, *76*, 957−963.
(10) Goswami, S.; Brady, J. E.; Jordan, D. A.; Li, G. *Anesthesiology* **2012**, *117*, 1018−1026.
(11) Ciccarone, D. *Curr. Opin. Psychiatry* **2021**, *34*, 344−350.
(12) Diversion Control Division. (2022). *National Forensic Laboratory Information System: NFLIS-Drug 2021 annual report*. U.S. Department of Justice, U.S. Drug Enforcement Administration.
(13) McQuay, H. J.; Moore, R. A.; Paterson, G. M. C.; Adams, A. P. *Br. J. Anaesth.* **1979**, *51*, 543−550.
(14) Day, J.; Slawson, M.; Lugo, R. A.; Wilkins, D. *J. Anal. Toxicol.* **2003**, *27*, 513−516.
(15) ARK/Randox. ARK fentanyl assay. https://www.ark-tdm.com/products/urine-drug-tests/fentanyl-II/index.html (accessed 2023-09-04).
(16) Neogen. Fentanyl Forensic ELISA Kit. https://www.neogen.com/categories/toxicology/fentanyl-forensic-elisa-kit/(accessed 2023-09-04).
(17) Lockwood, T.-L. E.; Vervoordt, A.; Lieberman, M. *Harm Reduct. J.* **2021**, *18*, 30.
(18) Ellington, A. D.; Szostak, J. W. *Nature* **1990**, *346*, 818−822.
(19) Tuerk, C.; Gold, L. *Science* **1990**, *249*, 505−510.
(20) Dunn, M. R.; Jimenez, R. M.; Chaput, J. C. *Nat. Rev. Chem* **2017**, *1*, 0076.
(21) Yu, H.; Alkhamis, O.; Canoura, J.; Liu, Y.; Xiao, Y. *Angew. Chem., Int. Ed.* **2021**, *60*, 16800−16823.
(22) Swensen, J. S.; Xiao, Y.; Ferguson, B. S.; Lubin, A. A.; Lai, R. Y.; Heeger, A. J.; Plaxco, K. W.; Soh, H. T. *J. Am. Chem. Soc.* **2009**, *131*, 4262−4266.

(23) Baker, B. R.; Lai, R. Y.; Wood, M. S.; Doctor, E. H.; Heeger, A. J.; Plaxco, K. W. *J. Am. Chem. Soc.* **2006**, *128*, 3138−3139.
(24) Ferguson, B. S.; Hoggarth, D. A.; Maliniak, D.; Ploense, K.; White, R. J.; Woodward, N.; Hsieh, K.; Bonham, A. J.; Eisenstein, M.; Kippin, T. E.; Plaxco, K. W.; Soh, H. T. *Sci. Transl. Med.* **2013**, *5*, 213ra165.
(25) Alkhamis, O.; Xiao, Y. *J. Am. Chem. Soc.* **2023**, *145*, 194−206.
(26) Canoura, J.; Wang, Z.; Yu, H.; Alkhamis, O.; Fu, F.; Xiao, Y. *J. Am. Chem. Soc.* **2018**, *140*, 9961−9971.
(27) Canoura, J.; Alkhamis, O.; Liu, Y.; Willis, C.; Xiao, Y. *Nucleic Acids Res.* **2023**, *51*, No. e19.
(28) Yang, K.-A.; Pei, R.; Stojanovic, M. N. *Methods* **2016**, *106*, 58−65.
(29) Yang, W.; Yu, H.; Alkhamis, O.; Liu, Y.; Canoura, J.; Fu, F.; Xiao, Y. *Nucleic Acids Res.* **2019**, *47*, No. e71.
(30) Martin, M. *EMBnet J.* **2011**, *17*, 10−12.
(31) Alam, K. K.; Chang, J. L.; Burke, D. H. *Mol. Ther.—Nucleic Acids* **2015**, *4*, No. e230.
(32) Sievers, F.; Wilm, A.; Dineen, D.; Gibson, T. J.; Karplus, K.; Li, W.; Lopez, R.; McWilliam, H.; Remmert, M.; Söding, J.; Thompson, J. D.; Higgins, D. G. *Mol. Syst. Biol.* **2011**, *7*, 539.
(33) Alkhamis, O.; Yang, W.; Farhana, R.; Yu, H.; Xiao, Y. *Nucleic Acids Res.* **2020**, *48*, No. e120.
(34) Liu, Y.; Canoura, J.; Alkhamis, O.; Xiao, Y. *ACS Appl. Mater. Interfaces* **2021**, *13*, 9491−9499.
(35) Xiao, Y.; Lai, R. Y.; Plaxco, K. W. *Nat. Protoc.* **2007**, *2*, 2875−2880.
(36) Steel, A. B.; Herne, T. M.; Tarlov, M. J. *Anal. Chem.* **1998**, *70*, 4670−4677.
(37) Yu, H.; Canoura, J.; Guntupalli, B.; Lou, X.; Xiao, Y. *Chem. Sci.* **2017**, *8*, 131−141.
(38) Yang, K.-A.; Barbu, M.; Halim, M.; Pallavi, P.; Kim, B.; Kolpashchikov, D. M.; Pecic, S.; Taylor, S.; Worgall, T. S.; Stojanovic, M. N. *Nat. Chem.* **2014**, *6*, 1003−1008.
(39) Crooks, G. E.; Hon, G.; Chandonia, J.-M.; Brenner, S. E. *Genome Res.* **2004**, *14*, 1188−1190.
(40) Wang, Z.; Yu, H.; Canoura, J.; Liu, Y.; Alkhamis, O.; Fu, F.; Xiao, Y. *Nucleic Acids Res.* **2018**, *46*, No. e81.
(41) Liu, Y.; Yu, H.; Alkhamis, O.; Moliver, J.; Xiao, Y. *Anal. Chem.* **2020**, *92*, 5041−5047.
(42) Zadeh, J. N.; Steenberg, C. D.; Bois, J. S.; Wolfe, B. R.; Pierce, M. B.; Khan, A. R.; Dirks, R. M.; Pierce, N. A. *J. Comput. Chem.* **2011**, *32*, 170−173.
(43) Alkhamis, O.; Canoura, J.; Willis, C.; Wang, L.; Perry, J.; Xiao, Y. *J. Am. Chem. Soc.* **2023**, *145*, 12407−12422.
(44) Slavkovic, S.; Eisen, S. R.; Johnson, P. E. *Biochemistry* **2020**, *59*, 663−670.
(45) Vorlíčková, M.; Kejnovská, I.; Bednářová, K.; Renčiuk, D.; Kypr, J. *Chirality* **2012**, *24*, 691−698.
(46) Xiao, Y.; Lubin, A. A.; Heeger, A. J.; Plaxco, K. W. *Angew. Chem., Int. Ed.* **2005**, *44*, 5456−5459.
(47) McCloskey, K. L.; Garriott, J. C.; Roberts, S. M. *J. Anal. Toxicol.* **1978**, *2*, 110−112.
(48) Heltsley, R.; DePriest, A.; Black, D. L.; Crouch, D. J.; Robert, T.; Marshall, L.; Meadors, V. M.; Caplan, Y. H.; Cone, E. J. *J. Anal. Toxicol.* **2012**, *36*, 75−80.
(49) Chatterton, C. N.; Scott-Ham, M. *Forensic Sci. Int.* **2018**, *284*, 146−152.
(50) Yu, H.; Chen, Z.; Liu, Y.; Alkhamis, O.; Song, Z.; Xiao, Y. *Angew. Chem., Int. Ed.* **2021**, *60*, 2993−3000.
(51) Arroyo-Currás, N.; Somerson, J.; Vieira, P. A.; Ploense, K. L.; Kippin, T. E.; Plaxco, K. W. *Proc. Natl. Acad. Sci. U.S.A.* **2017**, *114*, 645−650.
(52) Downs, A. M.; Plaxco, K. W. *ACS Sens.* **2022**, *7*, 2823−2832.

https://doi.org/10.1021/acs.analchem.3c04104
Anal. Chem. 2023, 95, 18258−18267

Supporting information for:

Aptamer-Based Fentanyl Detection in Biological Fluids

Juan Canoura, Yingzhu Liu, Obtin Alkhamis and Yi Xiao*

Department of Chemistry, North Carolina State University, 2620 Yarbrough Drive, Raleigh, NC, USA, 27607.

*Corresponding author: yxiao34@ncsu.edu

Table of Contents

Table S1. DNA sequences used in this work.

Sequences ID	Sequence (5'–3')
DNA library	GGAGGCTCTCGGGACGAC (N30) GTCGTCCCGCCTTTAGGATTTACAG
Bio-cDNA	GTCGTCCCGAGAGCCATA-/3BioTEG/
Forward primer	GGAGGCTCTCGGGACGAC
Biotinylated-reverse primer	/5Biosg/-CTGTAAATCCTAAAGGCGGGACGAC
Illumina-FP	ACACTCTTTCCCTACACGACGCTCTTCCGATCT (N45) GGAGGCTCTCGGGACGAC
Illumina-RP	GACTGGAGTTCAGACGTGTGCTCTTCCGATCT (N43) CTGTAAATCCTAAAGGCGGGACGAC
E1	GGGACGACTGCTTGGGTAGGTCGGGCTTGGGTTCGGCGGTCGTCCC
E2	GGGACGACAAAATGGCAGCATTGGTGACGGAGTTGCTTGTCGTCCC
L1	GGGACGACAAAAATGGAAGCATTGGTTGTTGGTGCTTTGTCGTCCC
P1	GGGACGACAGCTTGGTTTGGTCGGGGTAGGGTTCGGATGTCGTCCC
P2	GGGACGACTAATGGGAGCATTGGTCCACGCAGTGTGCAGTCGTCCC
P4	GGGACGACGGTTGGCTTGGGGTCGGGTGTGGGTGCGGCGTCGTCCC
P5	GGGACGACTGCTTGGGTAGGTCGGGTTTGGGTTCGGCGGTCGTCCC
E2-34	ACAAAATGGCAGCATTGGTGACGGAGTTGCTTGT
E2-34-MB	/ThiolC6/ ACAAAATGGCAGCATTGGTGACGGAGTTGCTTGT-/MB/

N = random nucleotides; /5Biosg/ = biotin tag; /3BioTEG/ = biotin tag with extended triethylene glycol linker; /ThiolC6/ = thiol group with six-carbon spacer; /MB/ = methylene blue redox tag

Table S2. Selection strategy and conditions for isolating fentanyl-binding aptamers via SELEX.

Round	**Pool (pmol)**	**Wash A (# washes)**	**Counter SELEX**	**Wash B (# washes)**	**Target (μM)**
1	1,000	10	As described in **Table S3**	N/A	100
2	350	20		30	100
3	350	20		30	100
4	300	40		40	50
5	300	40		40	50
6	300	40		40	50
7	300	40		40	50
8	300	40		40	50
9	300	40		40	50
10	300	40		40	50
11	300	40		40	10
12	300	40		40	5
13	300	40		40	5

Wash A and B were performed before and after counter-SELEX, respectively. 250 μL selection buffer was used for each wash.

Table S3. Selection conditions for counter-SELEX.

R	Counter-SELEX (# of total washes specified if >3)										
1	N/A										
2	A	B	C	D	E	K	L	M	N	G1	G2	G3
3	F	G	H	I	J	K	L	M	N	G1	G2	G3
4	A (×6)	B (×6)	C (×6)	D	E	K	L	M	N	G1(×6)	G2	G3
5	F (×6)	G (×6)	H (×6)	I	J	K	L	M	N	G1(×6)	G2	G3
6	A (×12)	B (×12)	C (×12)	D	E	K	L	M	N	G1(×6)	G2	G3
7	F (×12)	G (×12)	H (×12)	I	J	K	L	M	N	G1(×6)	G2	G3
8	A (×12)	B (×12)	C (×12)	D	E	K	L	M	N	G1(×12)	G2	G3
9	F (×12)	G (×12)	H (×12)	I	J	K	L	M	N	G1(×12)	G2	G3
10	A (×12)	B (×12)	C (×12)	D	E	K	L	M	N	O P Q R S T U V W		
11	F (×12)	G (×12)	H (×12)	I	J	K	L	M	N	O P Q R S T U V W		
12	M (×24)	D (×24)	A (×12)	B (×12)	C (×12)	E (×12)	F (×12)	G (×12)	H I J K L N O P Q R S T U V W			
13	M (×24)	D (×24)	A (×12)	B (×12)	C (×12)	E (×12)	F (×12)	G (×12)	H I J K L N O P Q R S T U V W			

A = Clomipramine; B = Citalopram; C = Alprazolam; D = Methylphenidate; E = Methadone; F = Amoxapine; G = Lorazepam; H = Clonazepam; I = (+)-Amphetamine; J = Tramadol; K = Quinine; L = Chlorpromazine; M = Procaine; N = (+)-Methamphetamine; O = Diphenhydramine; P = Lidocaine; Q = Benzocaine; R = Cocaine; S = Heroin; T = Ethylone; U = Naloxone; V = Naltrexone; W = Oxycodone; G1 = Diphenhydramine, lidocaine, and benzocaine; G2 = Cocaine, heroin, and ethylone; G3 = Naloxone, naltrexone, and oxycodone.

All counter-targets were prepared in 1× SELEX buffer except clomipramine, citalopram, alprazolam, amoxapine, lorazepam, and clonazepam, which included 1% MeOH as a co-organic solvent. During rounds 2 and 3, all counter-target concentrations were 100 µM. From rounds 4–13, the concentration of each counter-target was increased to 250 µM, except for clomipramine, citalopram, alprazolam, amoxapine, lorazepam, and clonazepam, which were kept at 100 µM. Each wash consisted of 250 µL of SELEX buffer. Each counter-target underwent three washes unless otherwise specified in the table. Between each counter-target, three washes with SELEX buffer were performed.

Table S4. Aptamer dissociation constants (K_D), and ITC experiment conditions.

Aptamer	Fentanyl (µM)	Aptamer (µM)	ΔH (kcal/mol)	ΔS (cal/mol/K)	K_D (nM)
E1	100	10	-22.5 ±0.1	-43.5	79 ± 7
E2	200	20	-16.2 ± 0.1	-23.5	143 ± 13
L1	200	20	-20.3 ± 0.1	-39.3	426 ± 20
P1	200	20	-30.64 ±0.1	-71.4	97 ± 6
P2	400	40	-17.3 ±0.07	-28.7	268 ± 8
P4	200	20	-30.7 ± 0.1	-70.3	49 ± 3
P5	200	20	-26.1 ±0.07	-56.7	128 ± 5

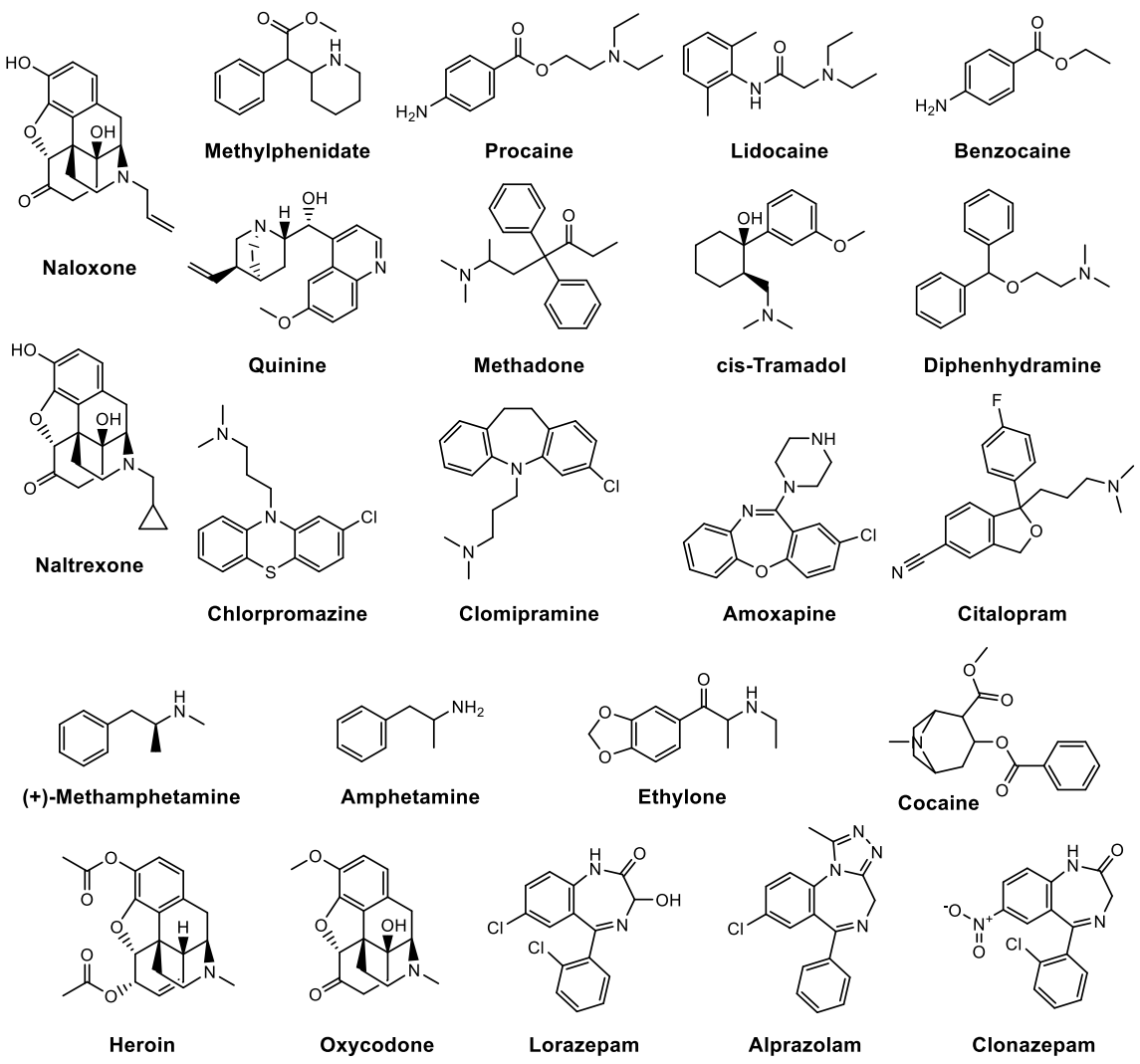

Figure S1. Chemical structures of interferents employed in counter-SELEX.

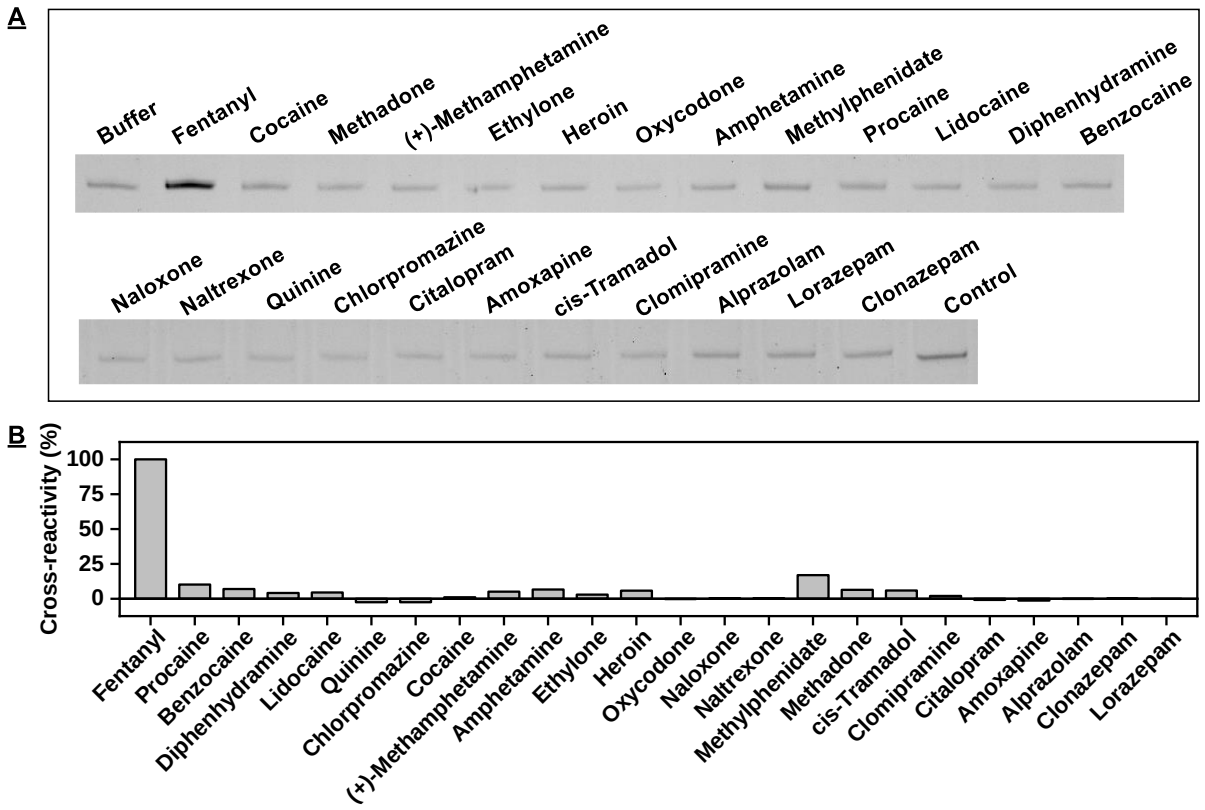

Figure S2. Specificity of the round 10 pool determined by gel elution assay. (**A**) Polyacrylamide gel electrophoresis (PAGE) results depict the ligand elution profile, with lanes representing samples of the pool eluted with various ligands. This control lane contains the random library at a fixed concentration of 10 nM. (**B**) Cross-reactivity of the round 10 pool against 25 μM fentanyl; 250 μM procaine, (+)-methamphetamine, lidocaine, diphenhydramine, benzocaine, cocaine, ethylone, heroin, naloxone, naltrexone, oxycodone, methylphenidate, methadone, amphetamine, cis-tramadol, quinine, or chlorpromazine; or 100 μM clomipramine, citalopram, alprazolam, amoxapine, lorazepam, or clonazepam. Cross-reactivity is calculated relative to 25 μM fentanyl.

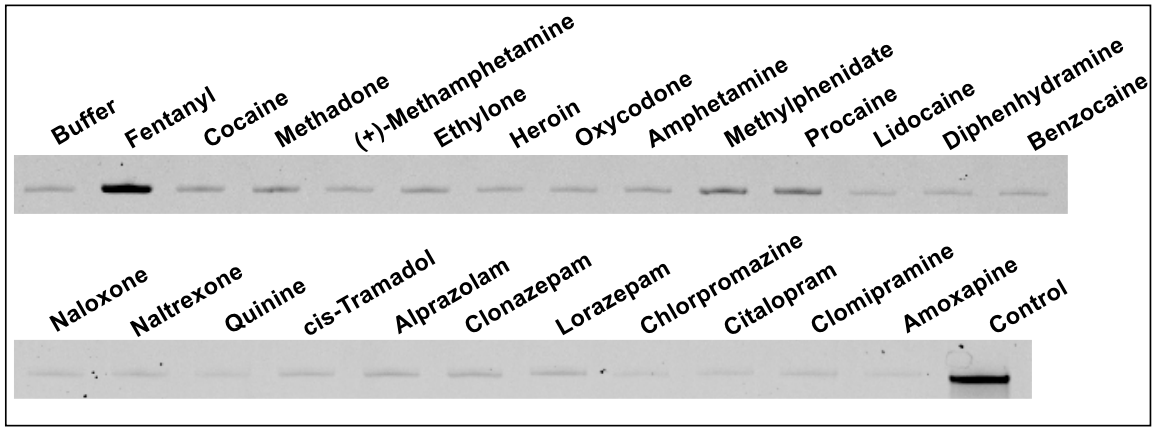

Figure S3. Specificity of the round 13 pool as determined by gel elution assay. PAGE results depict the elution profile obtained with various ligands. This control lane contains the random library at a fixed concentration of 30 nM.

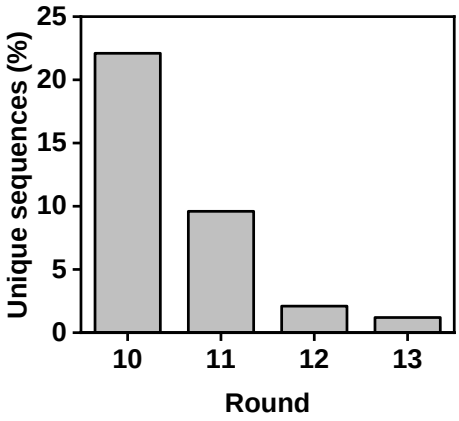

Figure S4. High-throughput sequencing (HTS) analysis of pool diversity (unique sequences) for rounds 10–13.

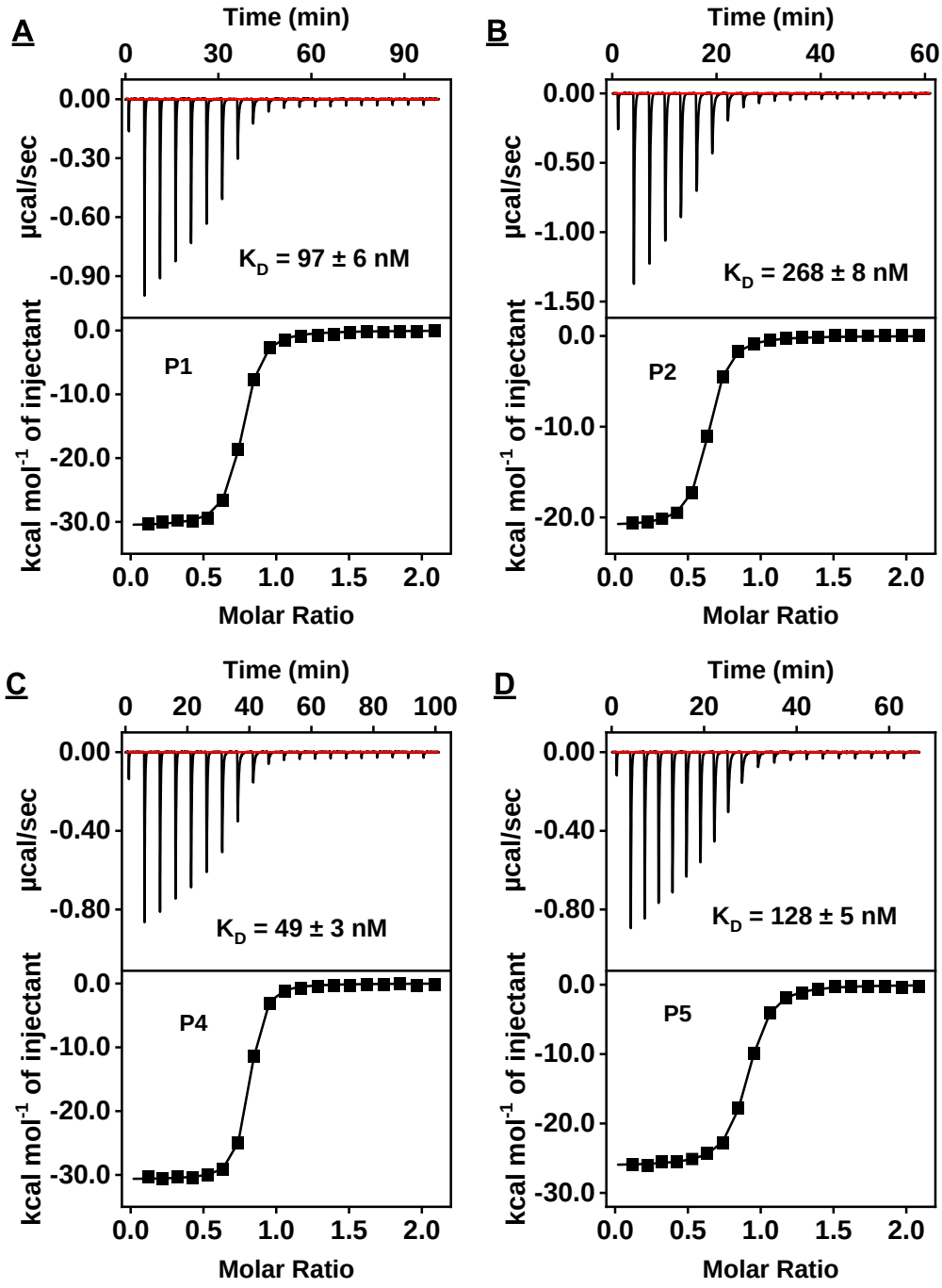

Figure S5. Characterization of fentanyl binding affinity of four aptamer candidates using ITC. The top panels display the heat generated from each titration of fentanyl into (**A**) P1, (**B**) P2, (**C**) P4, and (**D**) P5. Bottom panels show the integrated heat of each titration after correcting for the heat of dilution of the titrant.

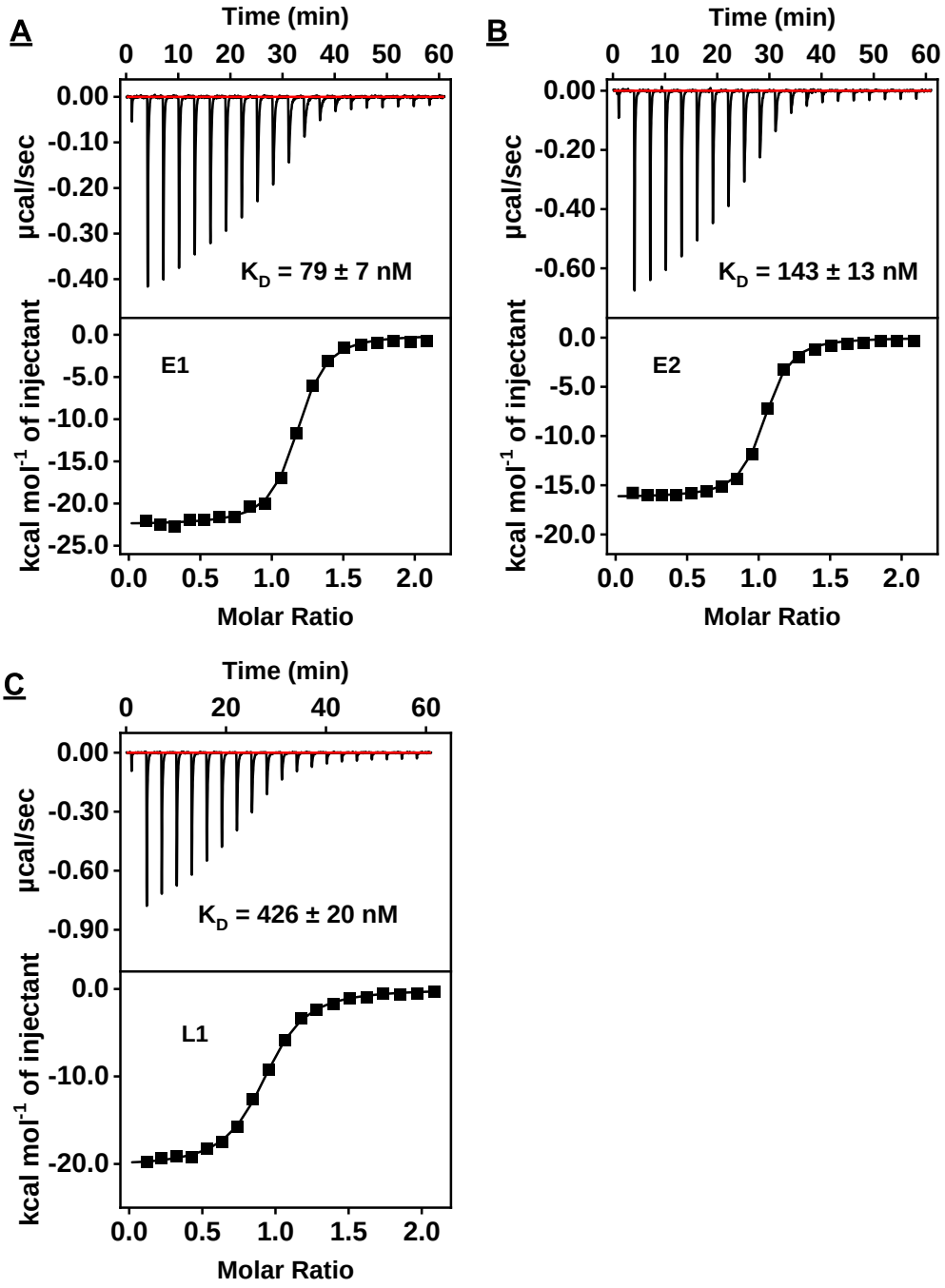

Figure S6. Characterization of fentanyl binding affinity of three aptamer candidates using ITC. The top panels display the heat generated from each titration of fentanyl into (**A**) E1, (**B**) E2, and (**C**) L1. Bottom panels show the integrated heat of each titration after correcting for the heat of dilution of the titrant.

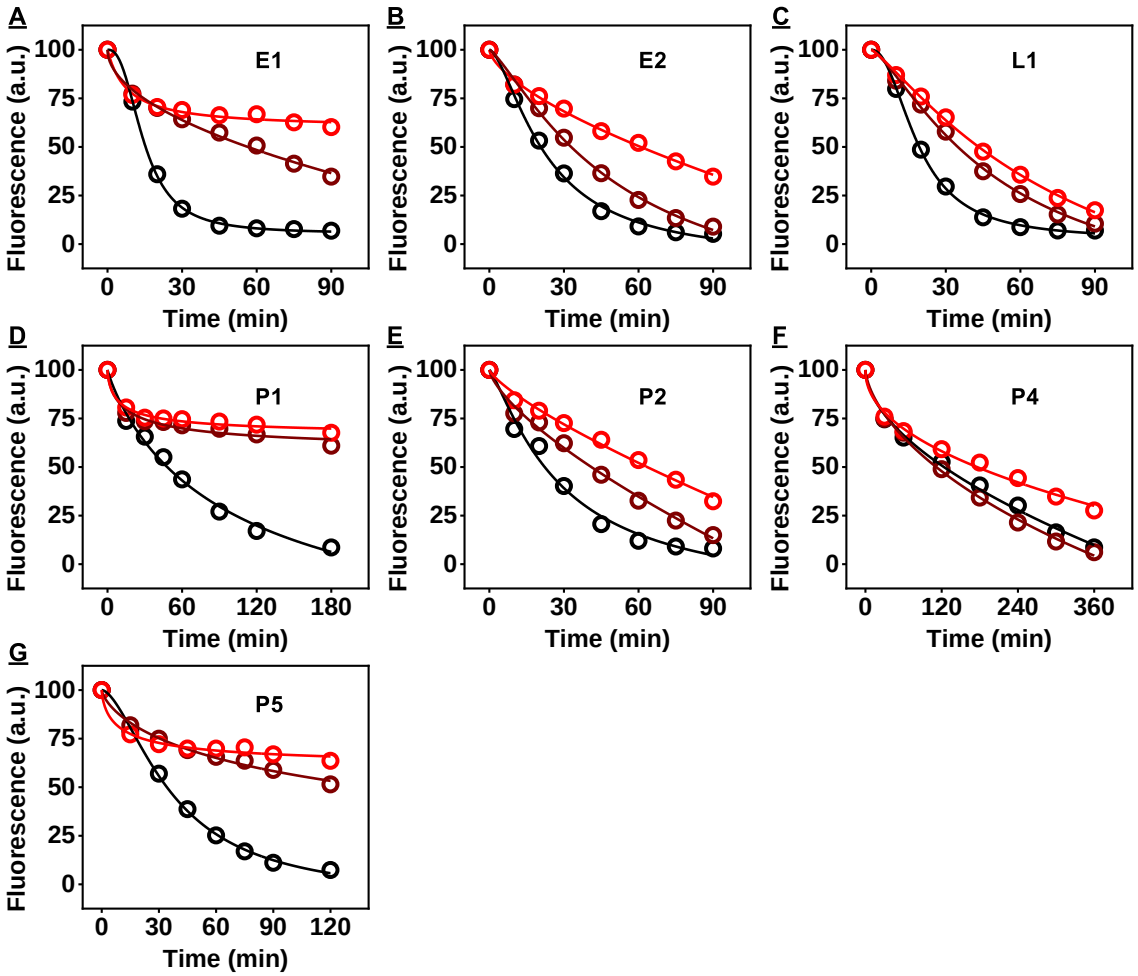

Figure S7. Exonuclease digestion time-course of fentanyl-binding aptamer candidates (**A**) E1, (**B**) E2, (**C**) L1, (**D**) P1, (**E**) P2, (**F**) P4, and (**G**) P5 in the presence of 0 (black), 25 (maroon), or 250 µM (red) fentanyl.

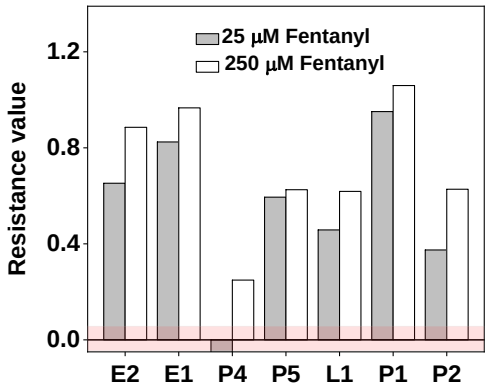

Figure S8. Resistance values of seven different aptamers in the presence of 25 µM or 250 µM fentanyl. The red-shaded area represents a resistance value of ± 0.05, which typically represents no ligand binding.

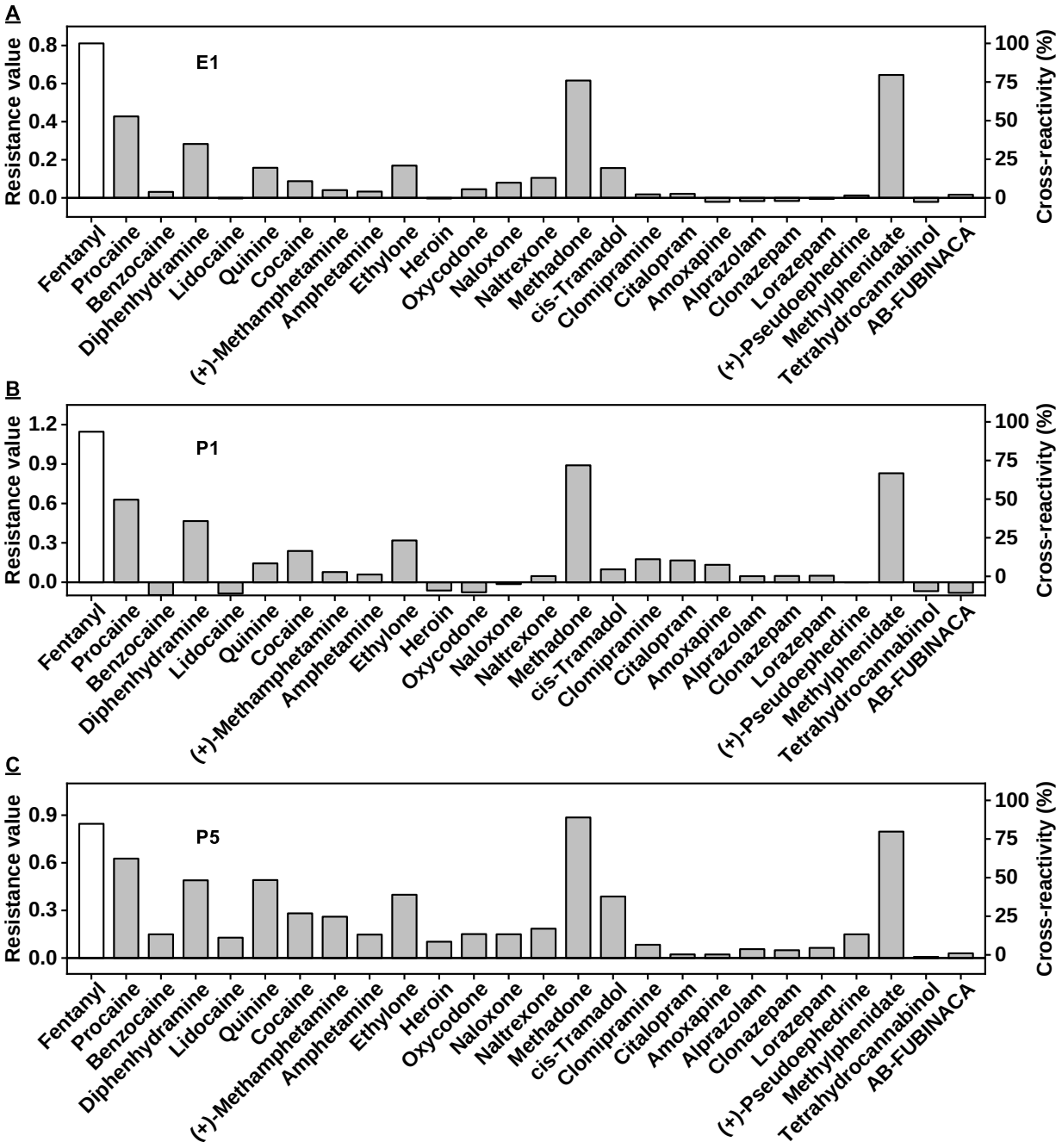

Figure S9. Screening the specificity of fentanyl-binding aptamers against interferents using an exonuclease digestion assay. Plots show resistance values obtained from time-course digestion of (**A**) E1, (**B**) P1, and (**C**) P5 in the presence of 25 μM fentanyl, tetrahydrocannabinol, and AB-FUBINACA; 50 μM clomipramine, citalopram, amoxapine, alprazolam, clonazepam, and lorazepam; or 250 μM other interferents.

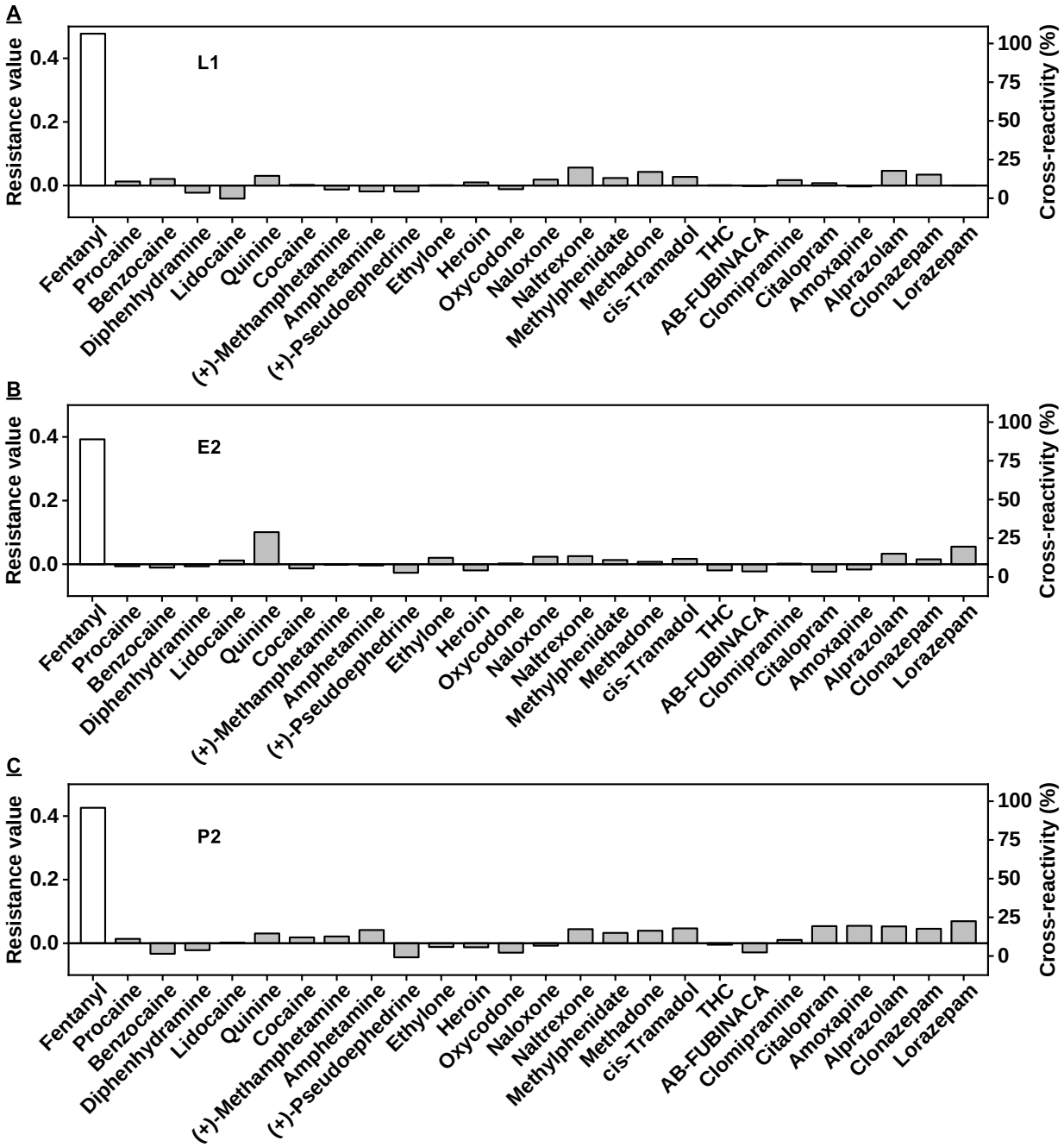

Figure S10. Screening the specificity of fentanyl-binding aptamers against interferents using an exonuclease digestion assay. Plots show resistance values obtained from time-course digestion of (**A**) L1, (**B**) E2, and (**C**) P2 in the presence of 25 μM fentanyl, tetrahydrocannabinol, and AB-FUBINACA; 50 μM clomipramine, citalopram, amoxapine, alprazolam, clonazepam, and lorazepam; or 250 μM other interferents.

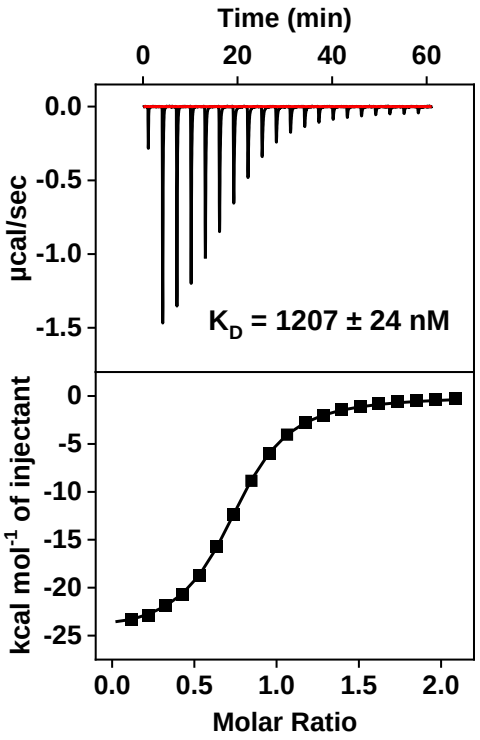

Figure S11. Characterization of fentanyl-binding affinity of E2-34 using ITC. Top panels display the heat generated from each titration of fentanyl into E2-34. Bottom panels show the integrated heat of each titration after correcting for the heat of dilution of the titrant.

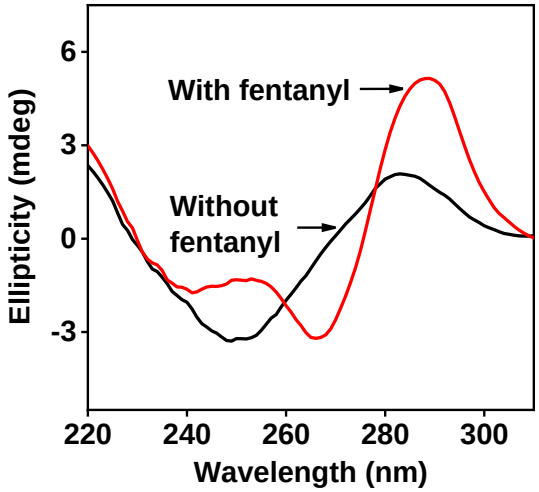

Figure S12. Circular dichroism spectra of E2-34 in the absence (black) and presence (red) of 10 µM fentanyl to confirm target-binding induced conformational change.

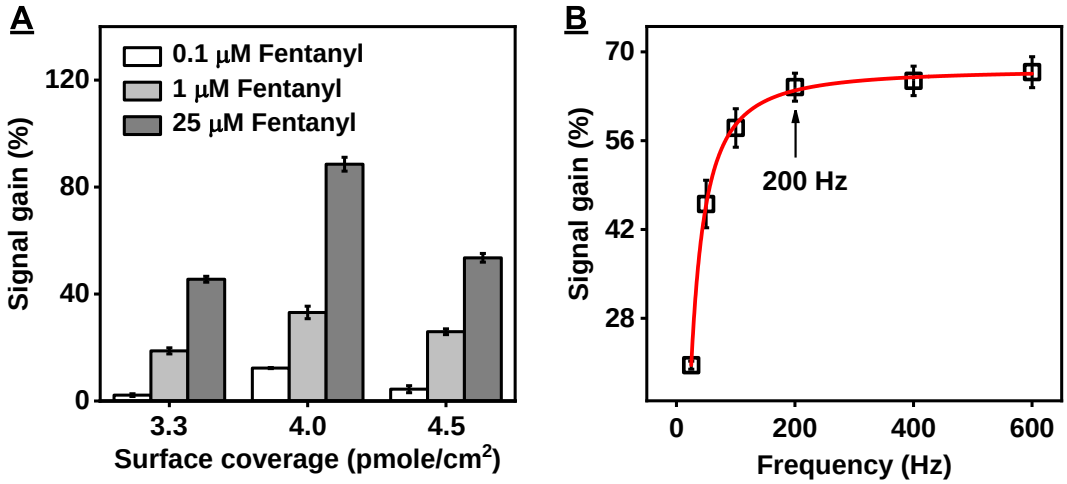

Figure S13. Optimizing analytical performance of E2-34-MB fabricated electrochemical aptamer-based (E-AB) sensors. (**A**) Optimization of aptamer surface density for detection of fentanyl. (**B**) Assessing signal gain from E-AB sensors modified with an optimal surface density of 4.0 pmol/cm^2 E2-34-MB at various square-wave voltammetry (SWV) frequencies for detection of 25 μM fentanyl. Error bars represent data from three independently fabricated electrodes.

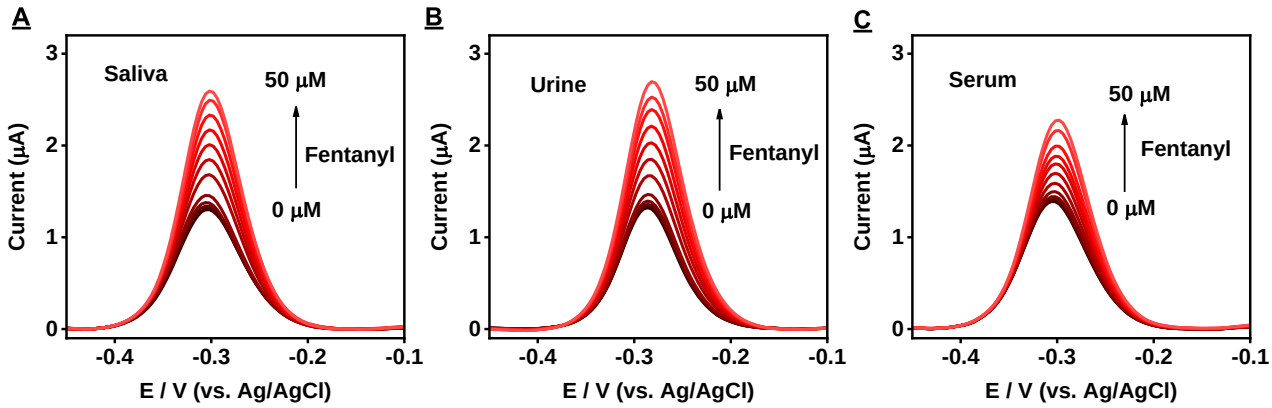

Figure S14. SWV data for E2-34-MB modified E-AB sensors in the presence of 0-50 μM fentanyl in (**A**) 50% saliva, (**B**) 50% urine and (**C**) 50% serum.

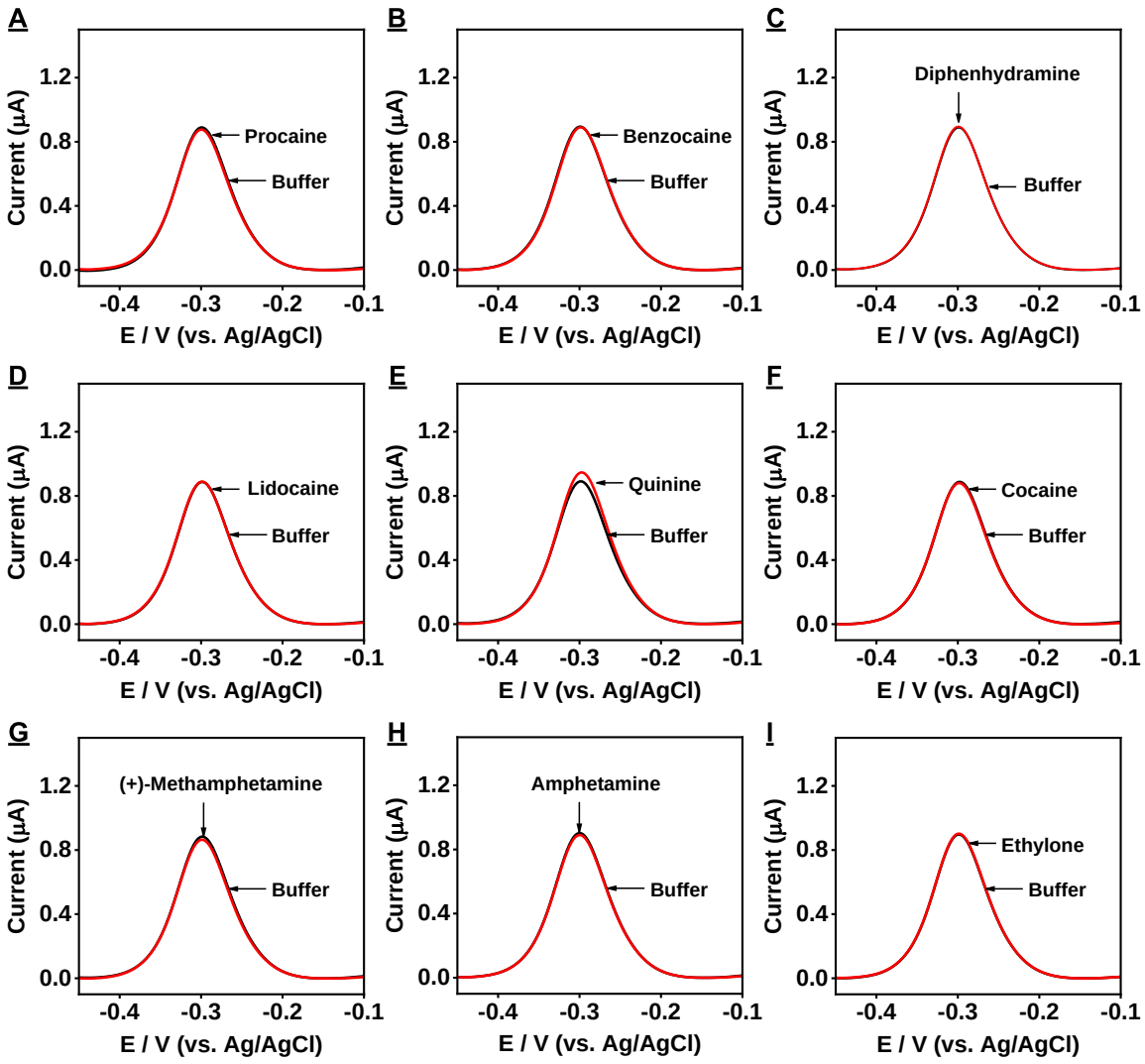

Figure S15. SWV spectra collected in buffer with (red) or without (black) 100 μM procaine, benzocaine, diphenhydramine, lidocaine, quinine, cocaine, (+)-methamphetamine, amphetamine, or ethylone using E2-34-MB-fabricated E-AB sensors.

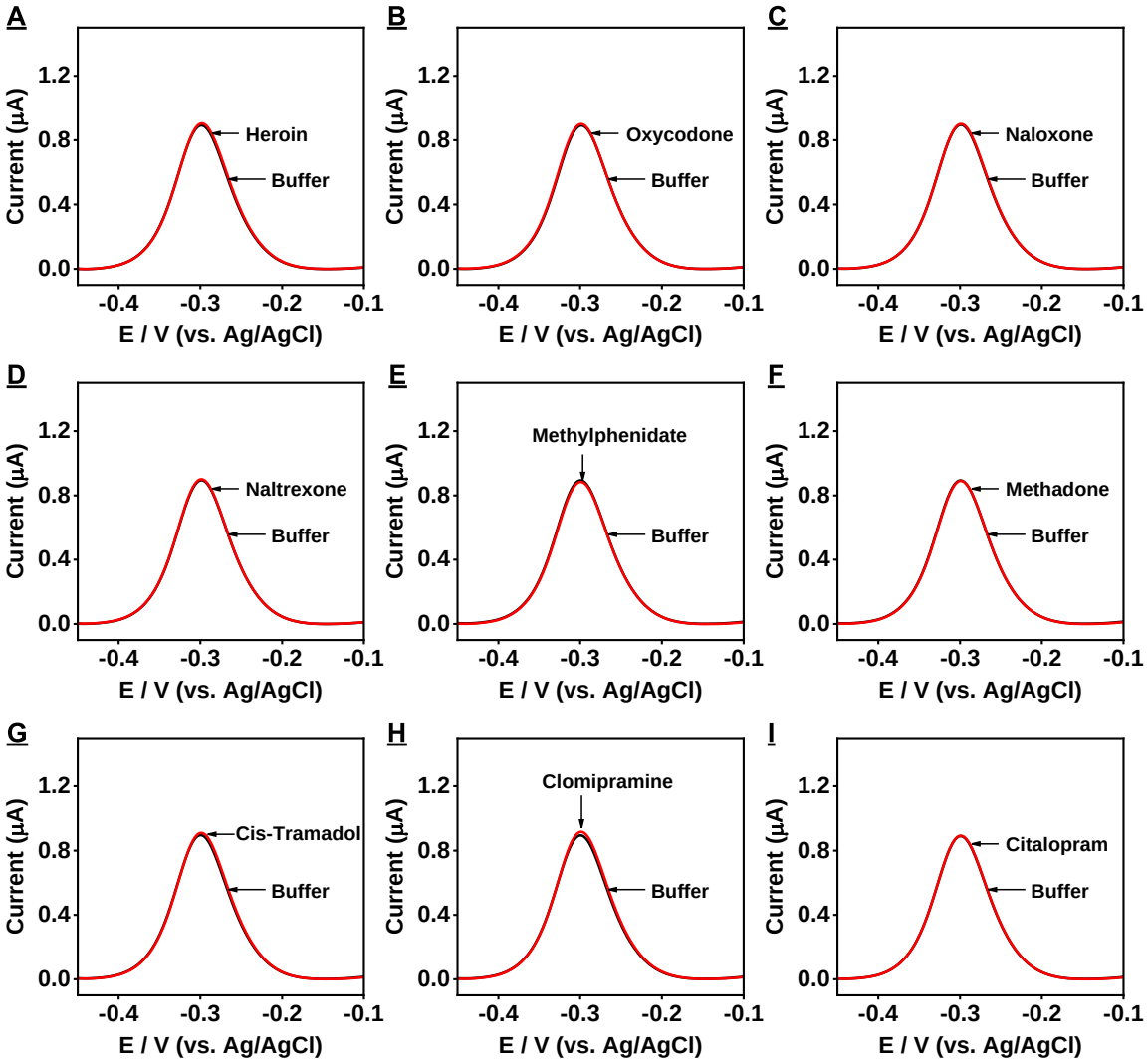

Figure S16. SWV spectra collected in buffer with (red) or without (black) 100 μM of heroin, oxycodone, naloxone, naltrexone, methylphenidate, methadone, or cis-tramadol, or 50 μM clomipramine or citalopram using E2-34-MB-fabricated E-AB sensors.

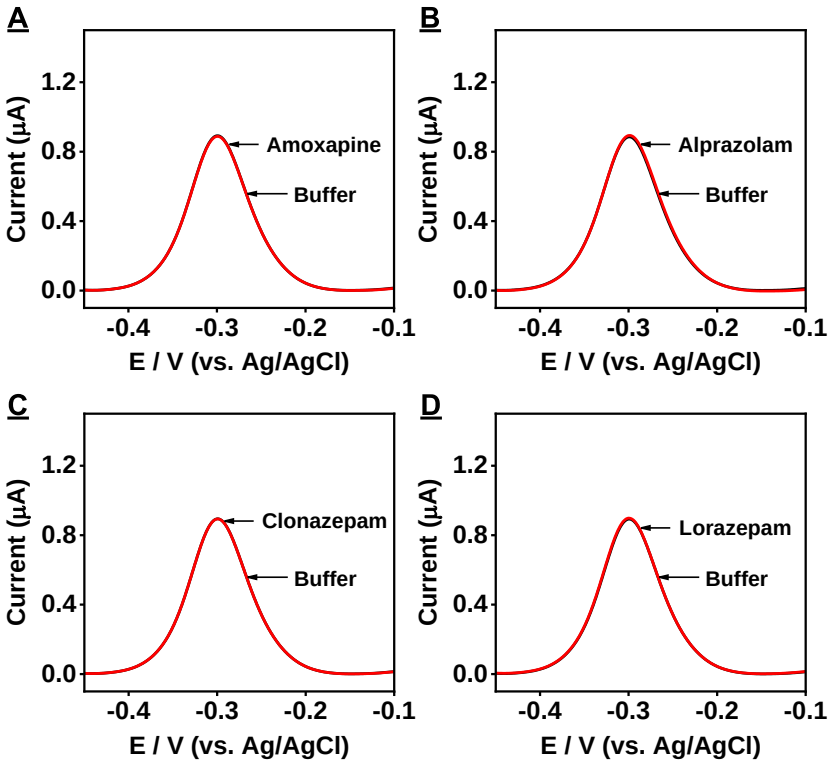

Figure S17. SWV spectra collected in buffer with (red) or without (black) 50 μM amoxapine, alprazolam, clonazepam, or lorazepam using E2-34-MB-modified E-AB sensors.